CHALMERS

Master Thesis

Design and Analysis of 60 kW DC-DC Converter for Hybrid Electric Vehicle Applications.

Students : Muhammad Rafiq
Mohammed Fareed Ul Hasan

Supervisor & examiner : Prof. Torbjörn Thiringer
Electric Power Engineering
Chalmers University of Technology, Göteborg

ABSTRACT

This thesis deals with the design and analysis of dc-dc converter with different core materials, core shapes, voltage levels and frequencies. The losses and efficiency of the converter is investigated. Furthermore the weight and losses of the converter are studied at different frequencies.

Analytical results shows that losses are higher in the 900 V system as compared to the 450V system.The analysis also shows that by increasing the operating frequency, the losses increases but the weight of the converter is reduced. A comparison of the two voltage level systems as proposed in the report shows that the two voltage systems behaves differently at different power losses but it is noted that the low voltage system is more energy efficient. The result suggests that the use of iron powder as core material reduces the weight of the converter. The result also shows that the core shape ETD-59 has smaller core losses as compared with the EC-70 core shape.

ACKNOWLEDGMENT

First, we would like to thank our examiner Professor Torbjörn Thiringer for his great help and support throughout our thesis work. We would like to thanks all the people in the department especially who helped us, Sonja Lundmark, Oskar Josefsson, Andreas Karvonen and Saeid Haghbin. At last but not the least, we would wish to thank the Jan-Olov Lantto which helped us a lot with our work station problems.

CONTENTS

ABSTRACT i
ACKNOWLEDGMENT ii
LIST OF SYMBOLS v
1 INTRODUCTION 1
1.1 Background 1
1.2 Purpose of work 1
2 SYSTEM OVERVIEW 3
2.1 The Hybrid Electrical Vehicle 3
2.2 Bidirectional boost converter 4
2.2.1 Generating mode 5
2.2.2 Motoring mode 7
3 SEMICONDUCTOR LOSS CALCULATION OF THE CONVERTER 11
3.1 IGBT and Diode Losses 11
3.1.1 Conduction Losses 11
3.1.2 Switching losses 13
4 BATTERY 15
4.1 The hybrid vehicle battery 15
4.2 Battery technology 15
4.3 Characteristics of Li-ion batteries 15
4.4 Charge 16
4.5 HEV Batteries 16
5 DESIGN 17
5.1 Design of the inductor 17
Parameters: 17
Core material, shape and size 17
5.2 Design of Capacitors 19
6 CASE SET UP 21
6.1 Base design 21
Converter parameters 21
6.1.1 Boost/Motoring mode 21
6.1.2 Buck/Generating mode 28

7 ANALYSIS 35
7.1 Mode of Operation 35
7.2 Core material 35
7.3 Core shape 35
7.4Voltage level 35
7.5 Switching frequency 35
Case 1.1: Ferrite material, (EC-70) for (450V System) 36
Case 1.2: Ferrite material, (ETD-59) for (450V System) 40
Case 1.3: Ferrite material, (EC-70) for (900V System) 42
Case 1.4: Ferrite material, (ETD-59) for (900V System) 44
Case 2.1: Iron powder material, (EC-70) for (450V System) 46
Case 2.2: Iron powder material, (ETD-59) for (450V System) 48
Case 2.3: Iron powder material, (EC-70) for (900V System) 50
Case 2.4: Iron powder material, (ETD-59) for (900V System) 52
8 CONCLUSION 57
REFERENCES 59

LIST OF SYMBOLS

D	*Duty Ratio of Switches*
$D_{1,2}$	*Diode*
R	*Resistor*
L	*Inductor of Converter*
I_L	*Inductor Current*
U_{in}	*Input voltage of the converter*
U_o	*output voltage of the converter*
f_{sw}	*Switching frequency of converter (Hz)*
t_{on}	*Switch on time (s)*
t_{off}	*Switch off time (s)*
T_{sw}	*Switching Time Period (1/ f_{sw})*
S	*Switch*
I_{in}	*Converter Input Current*
I_{load}	*Converter Load Current*
HEV	*Hybrid Electrical Vehicle*
P_o	*Output Power*

1 INTRODUCTION

1.1 Background

A critical factor propelling the shift from conventional gasoline/diesel engine vehicles to electric hybrid and fuel cell vehicles is the improvement in performance, size and cost of power electronics circuits over the past decade, with parallel improvements in sensors and microprocessors.

Typical power electronic circuits used in hybrid electric vehicles (HEV) include inverters and DC-DC converters. In some electrical vehicles the high voltage battery is connected directly to the inverters, however an alternate is to have a dc/dc converter in between to maintain a fixed dc voltage for the inverter. In this project we provide topology, design and analysis of this DC-DC converter for hybrid electrical vehicle applications (HEV).

1.2 Purpose of work

The purpose of this project is to design and analysis of a 60KW DC-DC converter for hybrid electric vehicle applications. This converter is able to maintain a constant DC link voltage when it is in motoring (or Up) mode of operation and energy flows from the DC voltage link bus to the battery when it works in generating (Down) mode of operation. The aim is to study the operation of the DC-DC converter at different switching frequencies respectively 10 and 20 kHz and different core materials with two different shapes for the inductor. The objective is to analyze losses and weight at different frequencies as well as analyze the efficiency at different power levels.

2 SYSTEM OVERVIEW

2.1 The Hybrid Electrical Vehicle

Figure 2.1 shows the block diagram of a HEV without DC-DC converter.

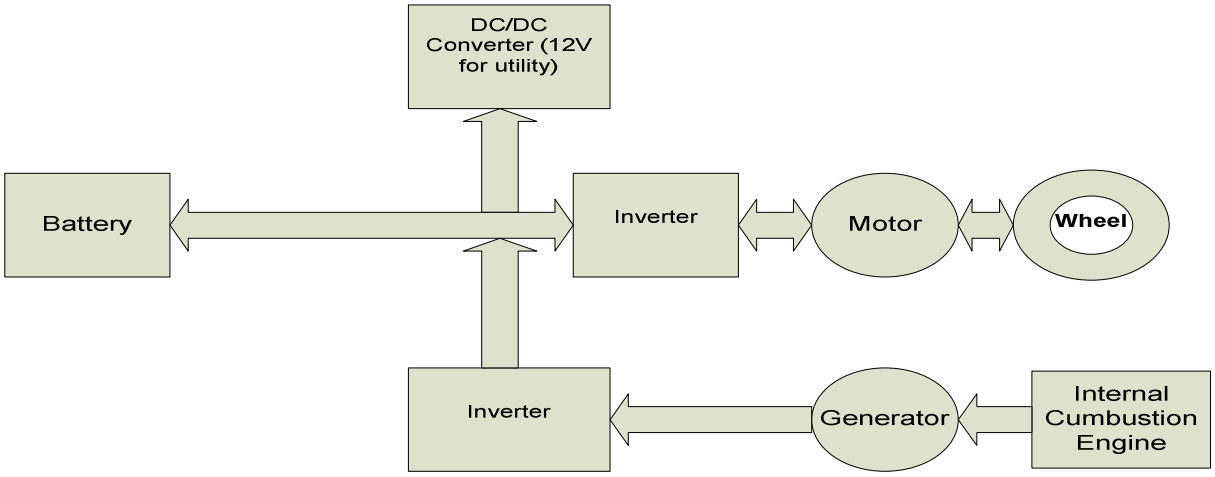

Figure 2.1. Block diagram of a HEV without DC-DC converter.

In Figute 2.1 shows the block diagram of a HEV with a battery directly connected to the inverter and further connected to the electric motor, and in the opposite direction power is transferred from Load (wheel-motor) to battery throgh inverter. In the other way the power comes from the generator to the inverter which is connected to the ICE.

Figure 2.2 shows the block diagram of a HEV without DC-DC converter.

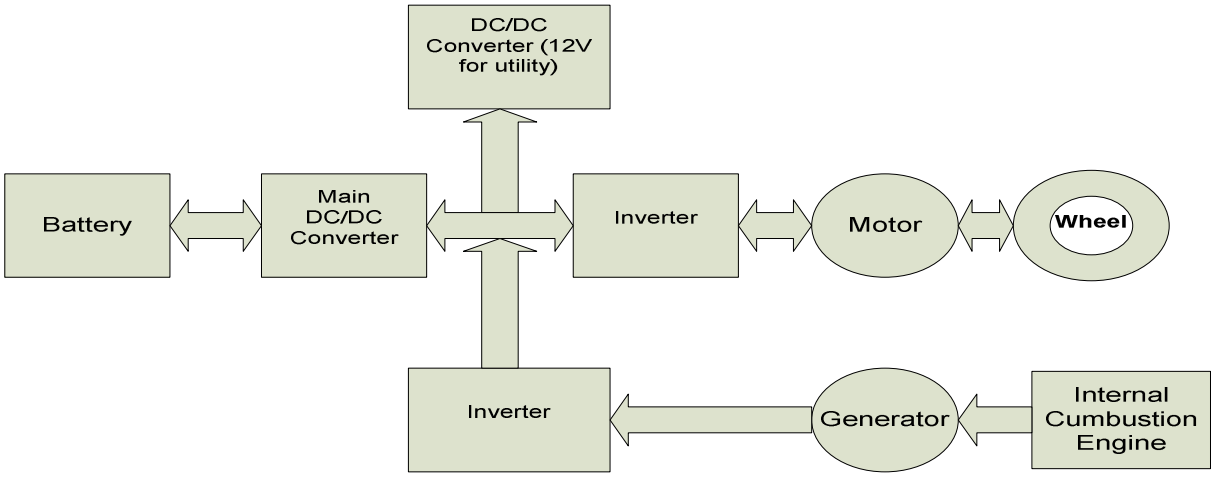

Figure 2.2. Block diagram of a HEV with DC-DC converter.

The DC-DC converter in a HEV is used to maintain a constant dc link voltage and to step up and step down the voltage as shown in Figure 2.2.

There are many different potential HEV configurations, but in general a HEV has an electric drive train like an EV, plus an internal combustion engine (ICE) that can charge the batteries periodically as is shown in Figure 2.2. The internal combustion engine is most efficient for a small range of operating conditions. This is utilized in HEV where the internal combustion engine can be made to operate at this efficient operating point. The HEV can operate the internal combustion engine (ICE) at its most efficient point for charging of the battery and can use the drive train to take up all the slack under other conditions. The emissions are lower than the combustion engine driving the car by itself and fuel economy can be significantly improved. The usable range of Electrical vehicles can be extended by hybrid technologies. A hybrid would allow the vehicle to operate in an urban/polluted area with only batteries and then switch to the engine outside the urban area.

2.2 Bidirectional boost converter

There are generally two bidirectional DC-DC converters in hybrid vehicle applications. One of them is a high-power converter that links the hybrid power train battery at a lower voltage with the high voltage DC bus. A second low-power converter links the hybrid battery with the low voltage auxiliary battery [1].

The operating principle of the DC-DC converter is shown in Figures 2.3.a-c.

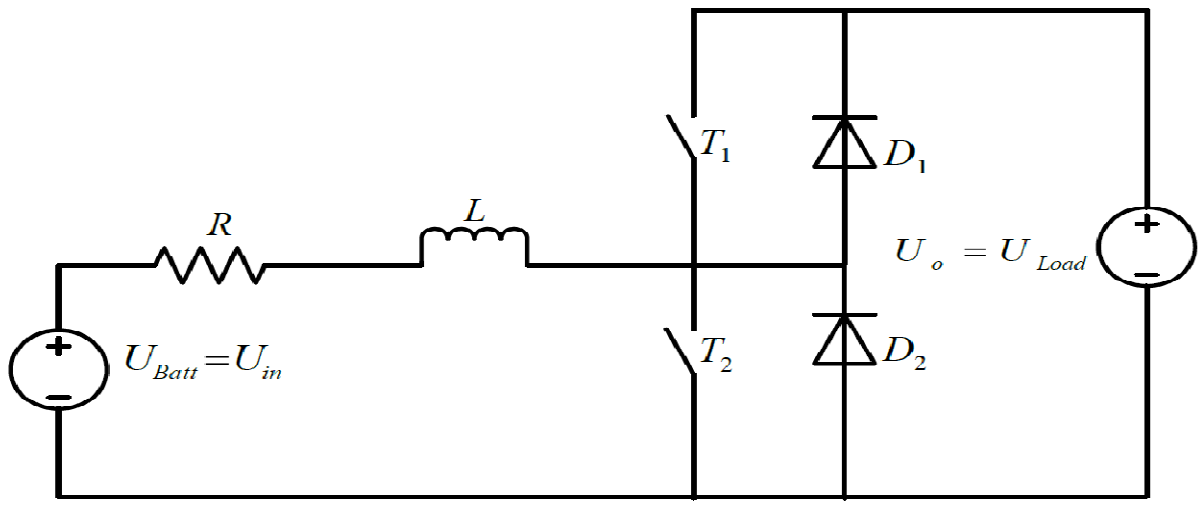

(a) Circuit topology of bidirectional converter

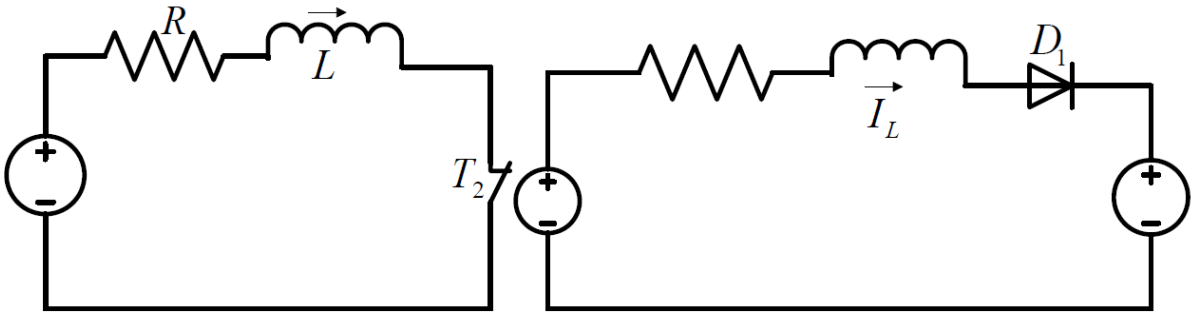

(b) Operating conditions for motoring mode of operation.

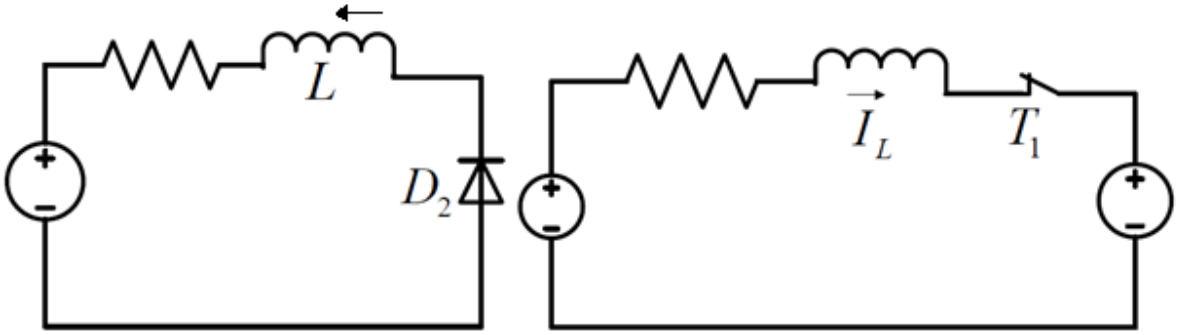

(c) Operating conditions for generating mode of operation.

Figure 2.3. Operation of the bidirectional boost converter.

In Figures 2.3 b-c shows the motoring and generating mode of a typical DC-DC converteris shown where in motoring mode the power is transfered from the battery to the load and vise versa.

2.2.1 Generating mode

In buck operation, as shown in Figure 1(c), the power is transferred from V_{load} to V_{batt}. When T_1 is closed and T_2 is open, since $V_{load} > V_{Battery}$, $V_L = V_{load} - V_{batt}$ and the inductor current I_L builds up. When T_1 is open, the inductor current I_L continues to flow through D_2. $V_L = -V_b$.

Assume ideal components and a constant V_o , the inductor current over one cycle in steady state operation will remain the same, e.g.

.

$$\int_{0}^{t1on}(V_{Battery}-V_{DCLink})dt=\int_{t1on}^{t1on+t1off}(-V_{DC\ Link}) \tag{2.1}$$

$$V_o=\frac{t1on}{T}V_{Battery}=D_1V_{Battery} \tag{2.2}$$

where D_1 is the duty ratio defined as the percentage of on-time of switch T_1

Parameters for loss calculation:

Figure 2 shows the typical signals in the step down (buck) converter. Input parameters for the calculation: Input voltage (U_{in}=V_{batt}), output voltage (U_o=V_{load}), output power (Po), inductor value (L), switching frequency (f_{sw}).
The output current of the converter is

$$I_o=\frac{P_o}{U_o} \tag{2.3}$$

The duty cycle in continuous conduction mode is

$$D=\frac{U_o}{U_{in}} \tag{2.4}$$

The output current ripple is

$$\Delta I_o=\frac{(1-D)U_o}{Lf_{sw}} \tag{2.5}$$

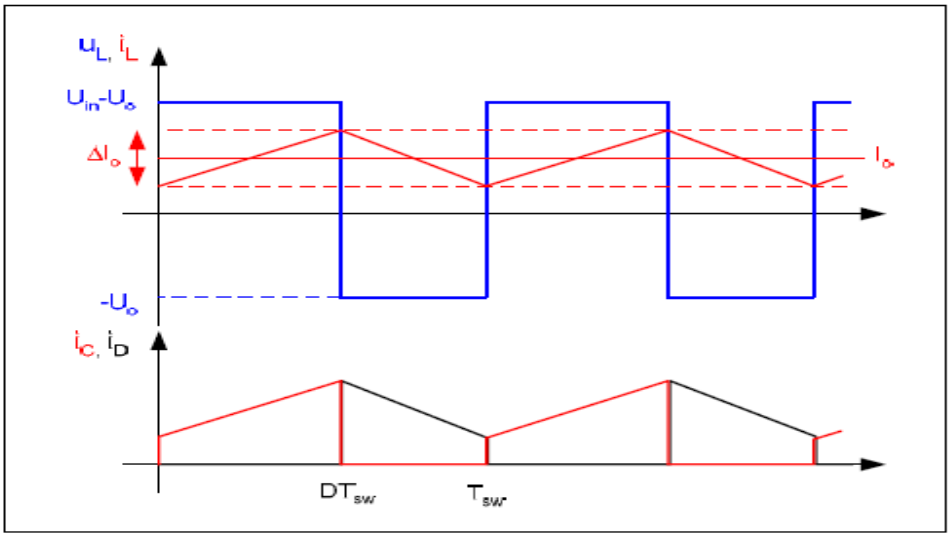

Figure 2.4. Inductor voltage, current, diode and capacitor current signals in generating mode.

In Figure 2.4 shows the typical signals of inductor voltage, inductor current, capacitor current, diode current input and output voltages.

The parameters needed for the loss calculation can be determined as

$$I_{con} = I_o - \frac{\Delta I_o}{2} \tag{2.6}$$

$$I_{coff} = I_o + \frac{\Delta I_o}{2} \tag{2.7}$$

$$I_{cav} = DI_o \tag{2.8}$$

$$I^2_{crms} = DI^2_o \tag{2.9}$$

$$I_{Dav} = (1-D)I_o \tag{2.10}$$

$$I^2_{Drms} = (1-D)I^2_o \tag{2.11}$$

2.2.2 Motoring mode

In this operation, the power is transferred from $V_{Battery}$ to V_{DC} Link. When T_2 is closed and T_1 is open, the output voltage capacitor and inductor form a direct path through switch T_2 as shown in Figure 1 (a &d). Therefore $V_L = -V_{Battery}$ and the inductor current I_L builds up. When T_1 is open, the inductor current continues to flow through D_1 to V_d, therefore $V_L = V_{DC\,Link} - V_{Battery}$.

Assume ideal components and a constant V_d, the inductor current over one cycle in steady state will remain the same, e.g.

$$\int_0^{t2on} (V_{DCLink})dt = \int_{t2on}^{t2on+t2off} (V_{Battery} - V_{DCLink})dt \tag{2.12}$$

$$V_{DCLink} = \frac{1}{1-D} V_{Battery} \tag{2.13}$$

where D is the duty ratio defend as the percentage of the on-time of switch T_2

$$D = \frac{t_{2on}}{T} \tag{2.14}$$

Parameters for loss calculation:

Figure 2.5 shows the typical signals in the step up (boost) converter. Input parameters for the calculation: Input voltage (*Uin=Vb*), output voltage (*Uo=Vd*), output power *(P*o), inductor value (*L*), switching frequency (f_{sw}).

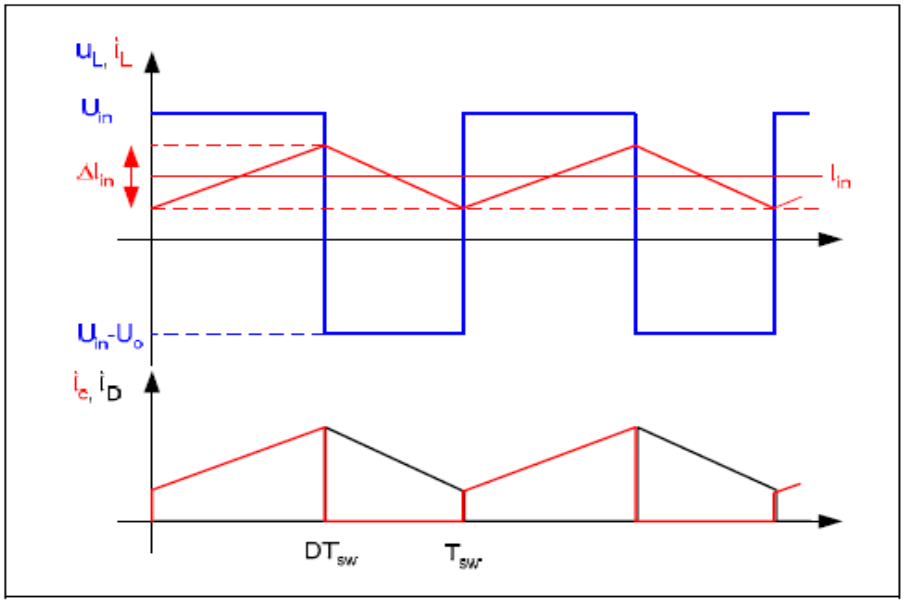

Figure 2.5. Inductor voltage, current, diode and capacitor current signals in motoring mode.

The input current is

$$I_{in} = \frac{P_{in}}{U_{in}} \tag{2.15}$$

where the duty cycle in continuous conduction mode is found to be

$$D = 1 - \frac{U_{in}}{U_o} \tag{2.16}$$

The input current ripple is

$$\Delta I_{in} = \frac{DU_{in}}{Lf_{SW}} \tag{2.17}$$

The parameters needed for the loss calculation can be determined as

$$I_{con} = I_{in} - \frac{\Delta I_{in}}{2} \tag{2.18}$$

$$I_{coff} = I_{in} + \frac{\Delta I_{in}}{2} \tag{2.19}$$

$$I_{cav} = D I_{in} \tag{2.20}$$

$$I^2_{crms} = (1-D) I_{in} \tag{2.21}$$

$$I_{Dav} = (1-D) I_{in} \tag{2.22}$$

$$I^2_{Drms} = (1-D) I^2_{in} \tag{2.23}$$

3 SEMICONDUCTOR LOSS CALCULATION OF THE CONVERTER

3.1 IGBT and Diode Losses

The IGBT and diode power losses as well as the power losses in any semiconductor component can be divided in three groups:

a) Conduction losses ($P_{conduction}$)
b) Switching losses (P_{sw})
c) Blocking leakage losses usually neglected

Therefore

$$P_{semicondutor} = P_{conduction} + P_{sw}$$

3.1.1 Conduction Losses

3.1.1 (a) IGBT conduction losses

The IGBT conduction losses can be calculated using an IGBT voltage drop behavior approximation with a series connection of a DC voltage source representing the IGBT on state zero current collector emitter voltage and collector on state resistance ($r_{C.}$) [2] as

$$u_{CE}(i_C) = u_{CE0} + r_C i_C \tag{3.1}$$

The important parameters can be read directly from the IGBT datasheet. The $u_{CE\,0}$ and values can be read from the diagram. The instantaneous value of the IGBT conduction losses are

$$P_{CT}(t) = u_{CE}(t) i_C(t) = u_{CE0} i_C(t) + r_C i^2{}_C(t) \tag{3.2}$$

The average IGBT current value is I_{cav} and value of IGBT current is I_{crms} . Then the average power losses can then be expressed as

$$P_{CT}(t) = \frac{1}{T_{SW}} \int_0^{T_{SW}} p(t)dt = \frac{1}{T_{SW}} \int_0^{T_{SW}} (u_{CE0} i_C(t) + r_C i_C{}^2(t)dt = u_{CE0} I_{cav} + r_C I_{crms}{}^2 \tag{3.3}$$

3.1.1 (b) Diode conduction losses

The same approximation can be used for the anti-parallel diode as is used for IGBT, giving

$$u_D(i_D) = u_{D0} + r_D i_D \tag{3.4}$$

The instantaneous value of the diode conduction losses is

$$P_{CD}(t) = u_D(t) i_D(t) = u_{D0} . i_F(t) + r_D i^2{}_D(t) \tag{3.5}$$

If the average diode current is I_{Dav} and the rms diode current is I_{Drms}, the average diode conduction losses across the switching period($T_{SW} = 1/f_{sw}$) are

$$P_{CD}(t) = \frac{1}{T_{SW}} \int_0^{T_{SW}} p(t)dt = \frac{1}{T_{SW}} \int_0^{T_{SW}} (u_{D0} i_D(t) + r_D i^2{}_D(t)dt = u_{D0} I_{Dav} + r_D I^2{}_{Drms} \tag{3.6}$$

The value of u_{CE0} and u_{D0} can be read from the datasheet as following. The r_C and r_D values can also be calculated from the datasheet by taking the slope of the desired line of characteristics as shown in Figure 3.1.

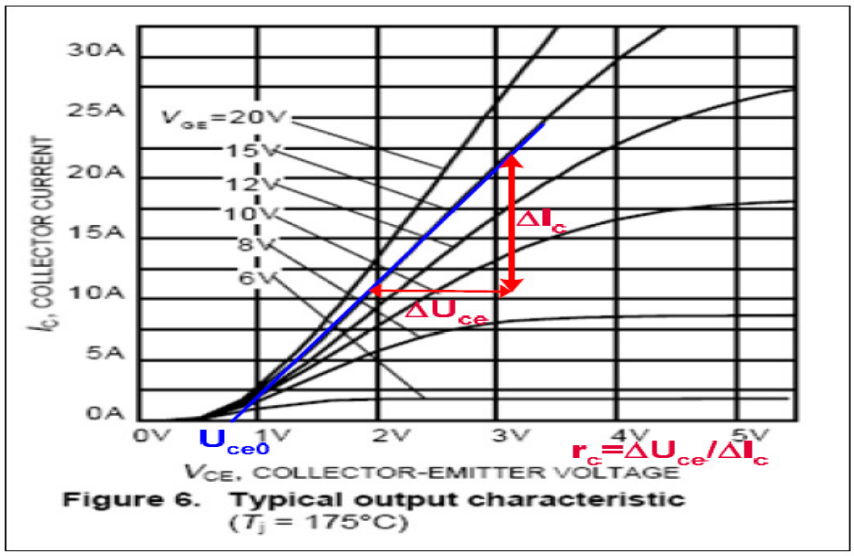

Reading the u_{CE0} and r_C ($r_C = \Delta U_{ce} / \Delta I_c$) from the data-sheet diagram

Figure 3.1. Shows how to read the initial voltage and resistance values from the graph of a transistor.

From Figure 3.1 can be seen that how to read the values of u_{CE0} and r_C .

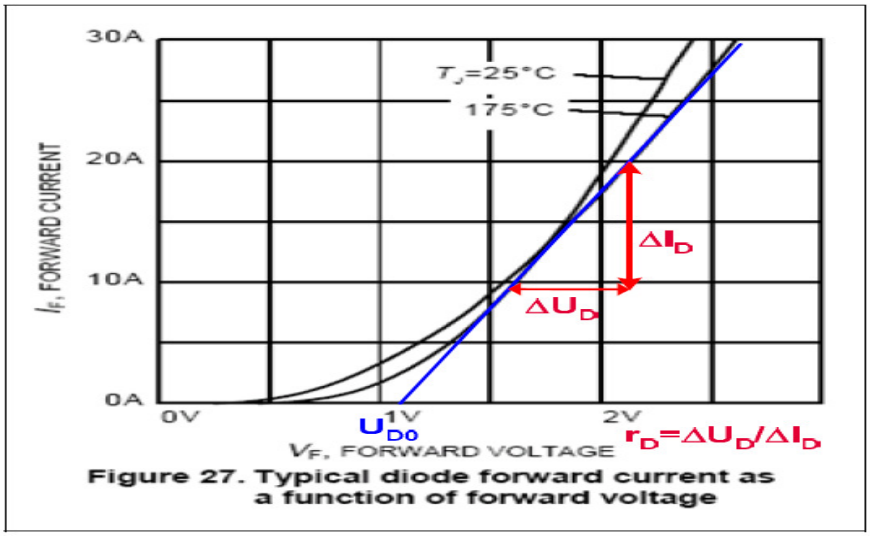

Figure 27. Typical diode forward current as a function of forward voltage

Reading the u_{D0} and r_D ($r_d = \Delta U_D / \Delta I_D$) from the data-sheet diagram

Figure 3.2 Shows how to read the initial voltage and resistance values from the graph of a diode.

From Figure 3.2 seen that how to read the values of u_{D0} and r_D .

3.1.2 Switching losses

The switching losses in the IGBT and the diode are the product of the switching energies and the switching frequency f_{sw}

$$P_{swM} = (E_{onM} + E_{offM}) f_{sw} \tag{3.7}$$

$$P_{swD} = (E_{onD} + E_{offD}) f_{sw} \tag{3.8}$$

where the energy during on and off period can be written as

$$E_{onM} = E_{refon} \frac{\Delta V_{in} I_{in}}{V_{ref} I_{ref}} \tag{3.9}$$

$$E_{offM} = E_{refoff} \frac{\Delta V_{in} I_{in}}{V_{ref} I_{ref}} \tag{3.10}$$

where V_{ref} and I_{ref} are taken from datasheet of IGBT and ΔV_{in} and I_{in} are the output voltage and current respectively.

E_{refon} and E_{refoff} can be calculated from the following typical switching losses of the IGBTaccording to Figure 3.3.

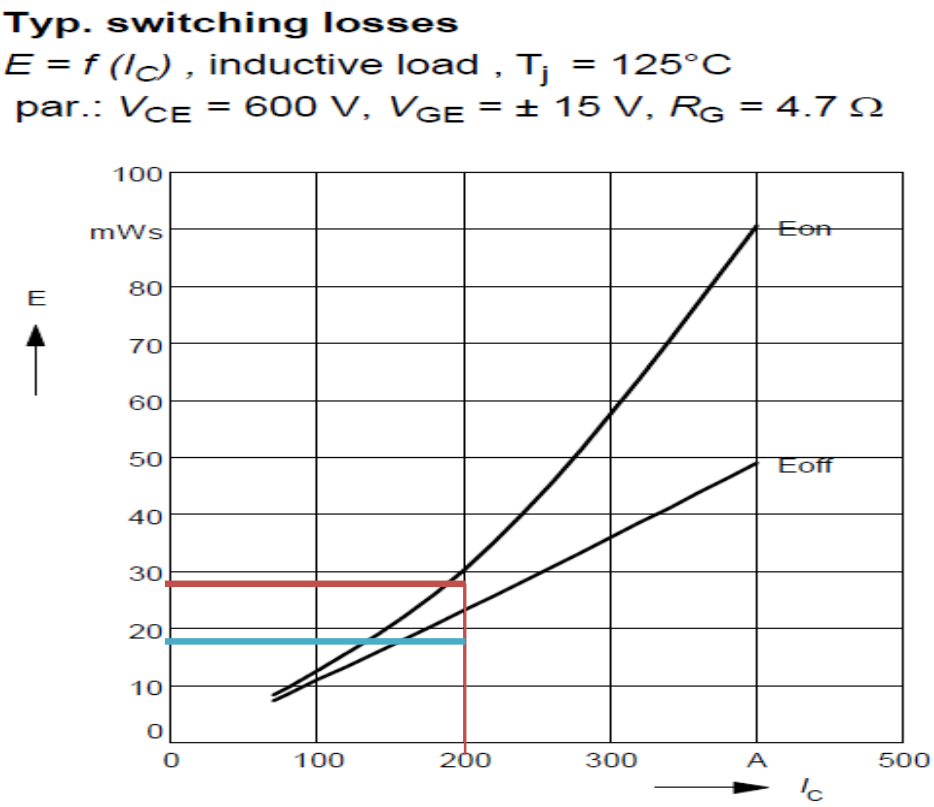

Figure 3.3. Shows how to read the energy values from the graph of a transistor.

Figure 3.3 show how to read the values of energies E_{onM} and E_{offM} can be read from a given datasheet at respective current level.

The turn on energy in the diode consists mostly of the reverse recovery energy (E_{onD})

$$E_{onD} = \frac{1}{4} Q_{rr} U_{Drr} \tag{3.11}$$

Where U_{Drr} is the voltage across the diode during reverse recovery. The Q_{rr} and U_{Drr} are taken from the datasheet of the IGBT.

Total losses

$$P_T = P_{CT} + P_{swT} = u_{CE0} I_{cav} + r_C I^2{}_{crms} + (E_{onT} + E_{offT}) f_{sw} \tag{3.12}$$

$$P_D = P_{CD} + P_{swD} = u_{D0} I_{Dav} + r_C I^2{}_{Drms} + E_{onD} f_{sw} \tag{3.13}$$

4 BATTERY

4.1 The hybrid vehicle battery

A hybrid vehicle battery is like any other battery except that it is always rechargeable and have power to propel a large heavy vehicle.

Hybrid vehicle batteries have two electrodes like other batteries (which collect or emit electric charge) which are lying in a ion rich solution called the electrolyte. The electrodes are separated from a thin polymer film called a separator which prevents them from touching [3].

A battery is actually a battery pack consisting of many individuals cells. A mobile phone battery is a single cell and a laptop battery consists of multiple cells working together.

4.2 Battery technology

The battery technology which is becoming most popular in hybrid electrical vehicles is the Li-ion (lithium-ion battery) technology.

4.3 Characteristics of Li-ion batteries

The battery voltage varies according to the kind of battery selected. For the DC/DC converter, the voltages used are between 300V and 400V. The peak power is selected to 60kW.

Small lithium ion batteries are widely used in notebook computers, mobile phones, cameras and other electronic equipment owing to their high energy density. Lithium cobalt oxide is used for anode in these small batteries but it is not used due to the high price of cobalt in large batteries used in vehicles. Lithium manganese oxide is used instead which is much cheaper. Manganese-based Li-ion batteries also have the following important characteristics for application to vehicles.

- Their charging/discharging efficiency and energy efficiency is high.
- A high single-cell voltage (three times that of Ni-MH batteries and twice that of lead-cid Batteries) which means less number of cells in the battery.
- The state of charge (SOC) can be sensed easily, so charging durations can be managed and driving ranges can be accurately predicted.

4.4 Charge

During discharging, lithium ions Li^+ carry the current from the negative to the positive electrode, through the non aqueous electrolyte and separator diaphragm [4].

During charging, an external electrical power source (the charging circuit) applies a higher voltage (but of the same polarity) than that produced by the battery, forcing the electrical current to pass in the reverse direction. The lithium ions then migrate from the positive to the negative electrode, where they become embedded in the porous electrode material in a process known as intercalation.

4.5 HEV Batteries

High output performance is a key component for HEV batteries. Large amount of regenerative breaking power make input (charging) performance equally important for truck, buses or other heavy duty HEVs. The specific energy, specific power, specific recharge power and battery capacity must be carefully established to match the output required by the motor, the regenerative breaking performance and hybrid system configuration (series or parallel) [5].

5 DESIGN

Inductors are not commercially available readymade for these power levels and it has to be designed for this particular application. In, this chapter, an inductor is designed [6].

5.1 Design of the inductor

Parameters:

The average current of the Inductor

$$I_{AVG} = \frac{P}{\Delta V_{in}} \tag{5.1}$$

The ripple current can be calculated as

$$\Delta I = \frac{I_{\max} - I_{\min}}{2} \tag{5.2}$$

where maximum and minimum currents can be calculated as

$$I_{\max} = I + \frac{0.2I}{2} \quad \text{and} \quad I_{\min} = I - \frac{0.2I}{2}$$

where switching frequency = f *(Hz)*

Inductance of the indutor = L *(μH)*

$$Z_{inductor} = 2\Pi fL \tag{5.3}$$

$$NI = \Phi R = \frac{\Psi}{N} R \tag{5.4}$$

$$NI = \frac{\Psi}{I} = \frac{N^2}{R} \tag{5.5}$$

Core material, shape and size

Effective area in square meters is = A_e

Effective length in meters is = l_e

Mass in grams = m

Volume in cubic meters = V_e

Relative permeability of the material = μ_r

Scaling factor = S_f

Permeability constant = μ_o

Current density = J (A/mm^2)

Reluctance for the iron part

$$R_{fe} = \frac{l_e}{\mu_o \mu_r A_e} \tag{5.6}$$

where air gap for coil = l_{air}

Reluctance for the air gap

$$R_{air} = \frac{l_{air}}{\mu_o \mu_r A_e} \tag{5.7}$$

The required number of turns

$$N = \sqrt{LR} \tag{5.8}$$

Total reluctance must be

$$R = R_{fe} + R_{air} \tag{5.9}$$

The total flux in the core can be calculated as

$$\Phi = \frac{NI}{R} \tag{5.10}$$

The total flux density in the core can be calculated as

$$B = \frac{\Phi}{A} \tag{5.11}$$

Conductor size can be calculated as

$$A_c = \frac{I_{in}}{J} \tag{5.12}$$

Change in flux density

$$\Delta B = \frac{N\Delta I}{RA_e} \tag{5.13}$$

The iron losses

$$P_{fe} = l_{factor} V_e \tag{5.14}$$

where B_{peak} and loss factor is obtained from datasheet.

Copper resistance

$$R_{cu} = \rho \frac{l_W}{A_c} \tag{5.15}$$

Winding length

$$l_w = NL_w \tag{5.16}$$

where turn length can be found from datasheet.

Copper losses

$$P_{cu} = R_{cu} I_{in}^{\ 2} \tag{5.17}$$

Total inductor losses

$$P_{total} = P_{fe} + P_{cu} \tag{5.18}$$

5.2 Design of Capacitors

Input capacitor (C_{Input}):

The C_{Input} can be calculated by the following formula

$$C_{Input} = \frac{\Delta I_L T_{sw}}{8\Delta V_o} \tag{5.19}$$

where $\Delta V_o$is peak-to-peak voltage ripple of the buck converter output (1 to 2 % of the output voltage).

Output capacitor (C_{Output}):

The C_{Output} can be calculated by the following formula

$$C_{Output} = \frac{I_o D T_{sw}}{\Delta V_o} \tag{5.20}$$

where ΔV_o is peak-to-peak voltage ripple of the boost converter output (1 to 2 % of the output voltage).

6 CASE SET UP

6.1 Base design

Converter parameters

P=60 kW

V_{input}*=300-400 V*

V_{output}*=450 V*

f =20 kHz

6.1.1 Boost/Motoring mode

The duty cycle is found as follows

$$D = 1 - \frac{\Delta V_{in}}{V_o} = 0.333 \tag{6.1}$$

The input current of the converter is

$$I_{in} = \frac{P}{\Delta V_{in}} = 200\ A \tag{6.2}$$

and the maximum and minimum current can be calculated as follows

$$I_{\max} = I_{in} + \frac{\Delta I_{in}}{2} = 220\ A \tag{6.3}$$

$$I_{\min} = I_{in} - \frac{\Delta I_{in}}{2} = 180\ A \tag{6.4}$$

and the ripple current can be found as

$$\Delta I = \frac{I_{\max} - I_{\min}}{2} = 20A$$

The average and rms currents of the IGBT and diode can be calculated as

The average current for IGBT is

$$I_{cav} = DI_{in} = 67\ A \tag{6.5}$$

and the rms current is

$$I_{crms} = \sqrt{D} I_{in} = 116\ A \tag{6.6}$$

The average current for diode is

$$I_{Dav} = (1-D) I_{in} = 134\ A \tag{6.7}$$

and rms current is

$$I_{Drms} = \sqrt{(1-D)} I_{in} = 164\ A \tag{6.8}$$

Conduction losses

If the average IGBT current value is I_{cav} and the rms value of IGBT current is I_{crms} as calculated above, then the average losses can be expressed as

$$P_{CT}(t) = u_{CE0} I_{cav} + r_C I_{crms}^{\ 2} = 120\ W \tag{6.9}$$

The values of u_{CE0} and r_C ($r_C = \frac{\Delta U_{CE}}{\Delta I_C}$) from the typical output characteristics

$I_C = f(U_{CE})$ taken from the IGBT data sheet. [7]

the conduction losses of a diode can be calculated as

$$P_{CD}(t) = u_{D0} I_{Dav} + r_D I^2_{Drms} = 145\ W \tag{6.10}$$

The value of u_{D0} can be read from the datasheet and r_D values can also be calculated from the datasheet by taking the slope of the desired line of characteristics.

Switching losses

The switching losses of the IGBT can be calculated using the E_{onT} and E_{offT} as

$$E_{onT} = E_{refon} \frac{\Delta V_{in} I_{in}}{V_{ref} I_{ref}} = 0.0043J \tag{6.11}$$

$$E_{offT} = E_{refoff} \frac{\Delta V_{in} I_{in}}{V_{ref} I_{ref}} = 0.0073J \tag{6.12}$$

where V_{ref} and I_{ref} are taken from datasheet of IGBT and V and I are the output voltage and current respectively.

$$P_{swT} = (E_{onT} + E_{offT}) f_{sw} = 234\ W \tag{6.13}$$

when the switching frequency at 20 kHz.

So the total IGBT losses are

$$P_T = P_{Conduction} + P_{SW} = 354\ W \tag{6.14}$$

The diode switching losses are

$$P_{swD} = (E_{onD} + E_{offD}) f_{sw} = 93\ W \tag{6.15}$$

where E_{onD} can be calculated as

$$E_{onD} = E_{Errref} \frac{\Delta V_{in} I_{in}}{V_{ref} I_{ref}} = 0.0047J \tag{6.16}$$

and the switch off losses in the diode are usually $(E_{offD} \approx 0)$ neglected, then the total diode losses are

$$P_D = P_{Conduction} + P_{SW} = 238\ W \tag{6.17}$$

So the total semiconductor losses are

$$P_{Semiconductor} = P_T + P_D = 59\ W \tag{6.18}$$

Design of the inductor for EC-70 core

Inductor average current I_{AVG} (A)	200
Current ripple ΔI (A)	20
Switching frequency f (kHz)	20
Inductance L (uH)	250
Air gap length l_{air} (mm)	10

Table 6.1. Ferrite EC-70

Reference	EC-70
Volume of the core (mm^3)	40100
Effective length of the core (mm)	144
Effective area of the core (mm^3)	279
Minimum are of the core (mm^3)	311
Mass of the core (g)	268
B_{sat} (T)	0.5

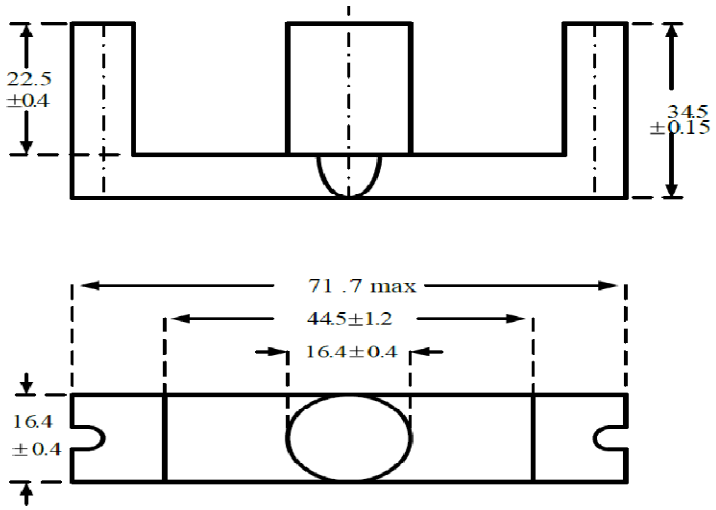

Figure 6.1. EC-70 core half, all dimensions in mm.

The above Figure 6.1 shows the EC-70 core half with all dimensions are in mm.

The winding area and the turn length is taken from datasheet is as

Winding area is = $\frac{465}{2} = 233\ mm^2$

Turn length $L_w = 97\ mm$

We have to scale the core according to our converter requirements so we will use a scale factor

Scaling factor $S_f = 3.49$

So with scaling factor the parameters of the core will be

$A_e = 3398\ mm^2$

$l_e = 5025\ mm$

$m = 11.39\ kg$

$V_e = 1704592\ mm^3$

Winding Area $A_W = 2831\ mm^2$

Turn length $L_w = 339.57 mm$

$\mu_o = 1.25 \times 10^{-6}$

Coil for 20A ripple current

Reluctance of iron part

$$\Re_{fe} = \frac{l_e}{\mu_o \mu_r A_e} = 1.5168 \times 10^6\ AT/Wb \tag{6.19}$$

Air gap length $l_{air} = 10\ mm$

Reluctance of air gap

$$\Re_{air} = \frac{l_{air}}{\mu_o \mu_r A_e} = 2.3542 \times 10^6\ AT/Wb \tag{6.20}$$

The total reluctance of the core is

$$\Re = \Re_{fe} + \Re_{air} = 3.8710 \times 10^6\ AT/Wb \tag{6.21}$$

Number of turns

$$N = \sqrt{LR} = 32 turns \tag{6.22}$$

Total flux

$$\Phi = \frac{NI_{in}}{\Re} = 0.0016\,Wb \tag{6.23}$$

Flux density

$$B = \frac{\Phi}{A_e} = 0.47T \tag{6.24}$$

Conductor size = $\frac{I_{in}}{3} = 66.67mm^2$ (6.25)

The required conductor area = $A_c = NA_{cond} = 2133mm^2$ (6.26)

Fill factor = $\frac{A_{cond}}{A_{wd}} = 0.73$ (6.27)

The flux density ripple can be calculated as

$$\Delta B = \frac{N\Delta I}{\Re A_e} = 0.04T \tag{6.28}$$

Inductor losses

The iron losses are

$$P_{fe} = l_{factor} V_e = 120\,W \tag{6.29}$$

where the 'lossfactor' l_{factor} is taken from the iron powder material graph at different frequencies [8].

Winding length $l_w = NL_w = 10.88m$ (6.30)

Copper resistance

$$R_{cu} = \rho \frac{l_w}{A_c} = 0.0028\ \Omega \tag{6.31}$$

Copper losses

$$P_{cu} = I^2{}_{in} R_{cu} = 377W \tag{6.32}$$

Total inductor losses

$$P_{inductor} = P_{fe} + P_{cu} = 496W \tag{6.33}$$

Filter losses

$$P_{Filter} = \Delta I^2 R = 3.2W \tag{6.34}$$

Total converter losses

$$P_{loss} = P_{Smiconductore} + P_{inductor} + P_{Filter} = 1090W \tag{6.35}$$

Efficiency of the converter at full load

$$\eta = \frac{P - P_{loses}}{P} = 98.18\ \% \tag{6.36}$$

6.1.2 Buck/Generating mode

Converter parameters:

$$P = 60\ kW$$

$$V_{input} = 450\ V$$

$$V_{output} = 300\ V$$

f_{sw} =20 kHz

The duty cycle is found as follows

The duty cycle is

$$D = \frac{\Delta V_o}{V_{in}} = 0.666 \tag{6.37}$$

The output current is

$$I_o = 150A$$

The ripple current can be found as

$$\Delta I = 15A$$

The value of inductance will be as follows

$$L = \frac{(1-D)\Delta V_o}{\Delta I \times f} = 340\,\mu H \tag{6.38}$$

Conduction losses

The average current of IGBT can be found as

$$I_{cav} = DI_o = 100\,A \tag{6.39}$$

The rms value of current for IGBT is as

$$I_{crms} = \sqrt{D} I_o = 122A \tag{6.40}$$

The average value of diode can be found as

$$I_{Dav} = (1-D)I_o = 50\,A \tag{6.41}$$

The rms value of current for diode can be found as

$$I_{Drms} = \sqrt{(1-D)}I_o = 87\,A \tag{6.42}$$

The conduction losses for IGBT are as follows

$$P_{CT}(t) = u_{CE\,0} I_{cav} + r_C I_{crms}^{\ 2} = 162\ W \tag{6.43}$$

And conducation losses for diode are

$$P_{CD}(t) = u_{D\,0} I_{Dav} + r_D I^{\,2}{}_{Drms} = 52\,W \tag{6.44}$$

The values of $u_{CE\,0}$ and r_C ($r_C = \frac{\Delta U_{CE}}{\Delta I_C}$) are taken from the typ. output characteristics

$I_C = f(U_{CE})$ of IGBT data sheet [7].

Switching losses

The E_{onT} and E_{offT} can be calculated as follows

$$E_{onT} = E_{refon} \frac{\Delta V_{in} I_{in}}{V_{ref} I_{ref}} = 0.0043\,J \tag{6.45}$$

and

$$E_{offT} = E_{refoff} \frac{\Delta V_{in} I_{in}}{V_{ref} I_{ref}} = 0.0073\,J \tag{6.46}$$

where V_{ref} and I_{ref} are taken from datasheet of IGBT and V and I are the output voltage and current respectively. The switching losses can be calculated as follows

$$P_{swT} = (E_{onT} + E_{offT}) f_{sw} = 233.34W \tag{6.47}$$

The diode switching losses are

$$P_{swD} = (E_{onD} + E_{offD}) f = 94W \tag{6.48}$$

where E_{onD} can be calculated as

$$E_{onD} = E_{Errref} \frac{\Delta V_{in} I_{in}}{V_{ref} I_{ref}} = 0.0047J \tag{6.49}$$

and the switch off losses in the diode are normally $(E_{offD} \approx 0)$ when the frequency 20 kHz.
So the total IGBT losses are

$$P_T = P_{Conduction} + P_{SW} = 396W \tag{6.50}$$

And the total diode losses are

$$P_D = P_{Conduction} + P_{SW} = 144W \tag{6.51}$$

So the total semiconductor losses are

$$P_{Semiconductor} = P_T + P_D = 540W \tag{6.52}$$

Capacitance calculation and filter losses

$$\Delta V_o = 0.02 V_o = 6V$$

The value of capacitance is

$$C_{in} = \frac{V(1-D)}{8 \Delta V_o f^2_{sw}} = 6.94 \mu F \tag{6.53}$$

So the filter losses are

$$P_{Filter} = \Delta I^2 R = 1.8W \tag{6.54}$$

Design of the inductor for EC- 70 core

Inductor average current $I_{AVG} = 150\,A$

Current ripple is $\Delta I = 15A$

Frequency $f_{sw} = 20\ kHz$

Inductance $L = 340\,\mu H$

Core material, shape and size

of the air gap l_{air}=10mm. The respective results were obtained.

The winding area and turn of length is taken from datasheet is as

Winding area is = $\frac{465}{2} = 233\ mm^2$

Turn length $L_w = 97.3\,mm$

We have to scale the core according to our converter requirements the available form of the core is too small for the converter.

Scaling factor $S_f = 3.3$

So with scaling factor the parameters of the core will be

The effective area for the core is $A_e = 3038.31 mm^2$

The effective length for the core is $l_e = 475.2mm$

Mass of core $m = 9.6311\ kg$

The effective volume is $V_e = 1.4411 \times 10^6 mm^3$

Winding Area $A_W = 2531\ mm^2$

Turn length $L_w = 321\ mm$

$\mu_o = 1.25 \times 10^{-6}$

Coil for 15A ripple current

Reluctance of iron part

$$\Re_{fe} = \frac{l_e}{\mu_o \mu_r A_e} = 1.60 \times 10^6 \, AT/Wb \tag{6.55}$$

Air gap length $l_{air} = 10\, mm$

Reluctance of air gap

$$\Re_{air} = \frac{l_{air}}{\mu_o A_e} = 2.633 \times 10^6 \, AT/Wb \tag{6.56}$$

The total reluctance can be written as

$$\Re = \Re_{fe} + \Re_{air} = 4.2372 \times 10^6 \, AT/Wb \tag{6.57}$$

The required number of turns

$$N = \sqrt{LR} = 26 turns \tag{6.58}$$

The total flux

$$\Phi = \frac{NI_{in}}{\Re} = 0.0009 Wb \tag{6.59}$$

The total flux density

$$B = \frac{\Phi}{A_e} = 0.291 T \tag{6.60}$$

Conductor size = $\frac{I_{in}}{3} = 50\, mm^2$ (6.61)

The required winding area

$$A_c = NA_{cond} = 1300\, mm^2 \tag{6.62}$$

Fill factor $= \frac{A_{cond}}{A_{wd}} = 0.35$

The flux density ripple

$$\Delta B = \frac{N\Delta I}{\Re A_e} = 0.029T \tag{6.63}$$

Inductor losses

The iron losses can be calculated as

$$P_{fe} = l_{factor} V_e = 87W \tag{6.64}$$

where the lossfactor l_{factor} is taken from the iron powder graph [8].

Winding length

$$l_w = NL_w = 8.3m \tag{6.65}$$

Copper resistance of the coil can be calculated as

$$R_{cu} = \rho \frac{l_w}{A_c} = 0.0090\,\Omega \tag{6.66}$$

Copper losses of the coil can be calculated as

$$P_{cu} = I^2{}_{in} R_{cu} = 204W \tag{6.67}$$

The total inductor losses can be calculated as

$$P_{inductor} = P_{fe} + P_{cu} = 290W \tag{6.68}$$

Filter losses can be calculated as

$$P_{Filter} = \Delta I^2 R = 1.8W \tag{6.69}$$

Total converter losses

$$P_{Total} = P_{Smiconduct\,ore} + P_{inductor} + P_{Filter} = 831W \tag{6.70}$$

Efficiency of the converter

$$\eta = \frac{P_{in} - P_{loss}}{P_{in}} = 98.61\% \tag{6.71}$$

7 ANALYSIS

In this chapter the results and plots for different voltage levels and two different core materials with two different core shapes will be presented.

7.1 Mode of Operation

- Motoring Operation
- Generating Operation

7.2 Core material

- Ferrite
- Iron powder (somaloy)

7.3 Core shape

- EC70/3C81
- ETD-59/3C90

7.4Voltage level

- 350-400-450
- 700-800-900

7.5 Switching frequency

- 5 kHz
- 10 kHz
- 20 kHz

Case 1.1: Ferrite material, (EC-70) for (450V System)

Motoring mode (Boost operation) when B=0.3 T, Lair=10 mm at 10 & 20 kHz:

In Figure 7.1 shows the switching and conduction losses of IGBT, diode, inductor losses and the efficiency plots at different loadings on different switching frequencies.

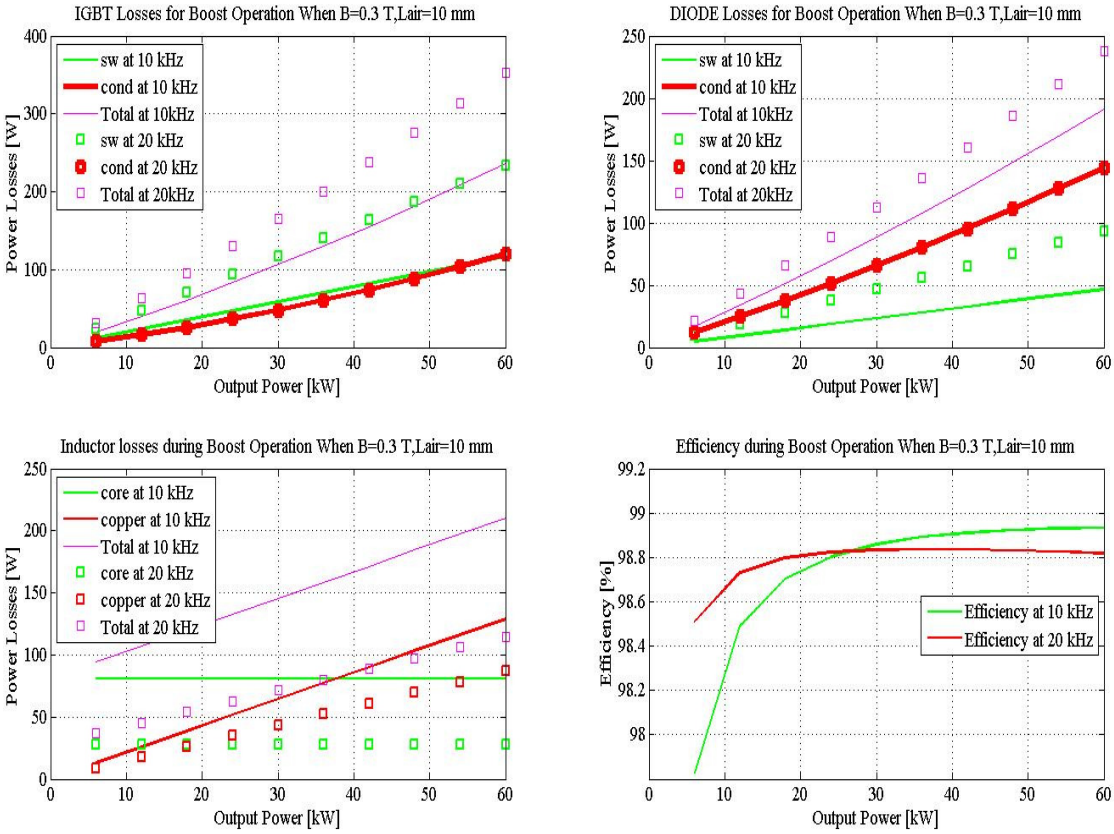

Figure 7.1. IGBT, diode, inductor losses and efficiency plots at different frequencies.

As can be seen from Figure 7.1, the switching losses are higher at 20 kHz in both the semiconductor devices, in an inductor the copper and core losses are higher at 10 kHz switching frequency and the efficiency varies from 98.8 to 98.88%.

In Figure 7.2, shows the total losses and weight of the converter at different switching frequencies.

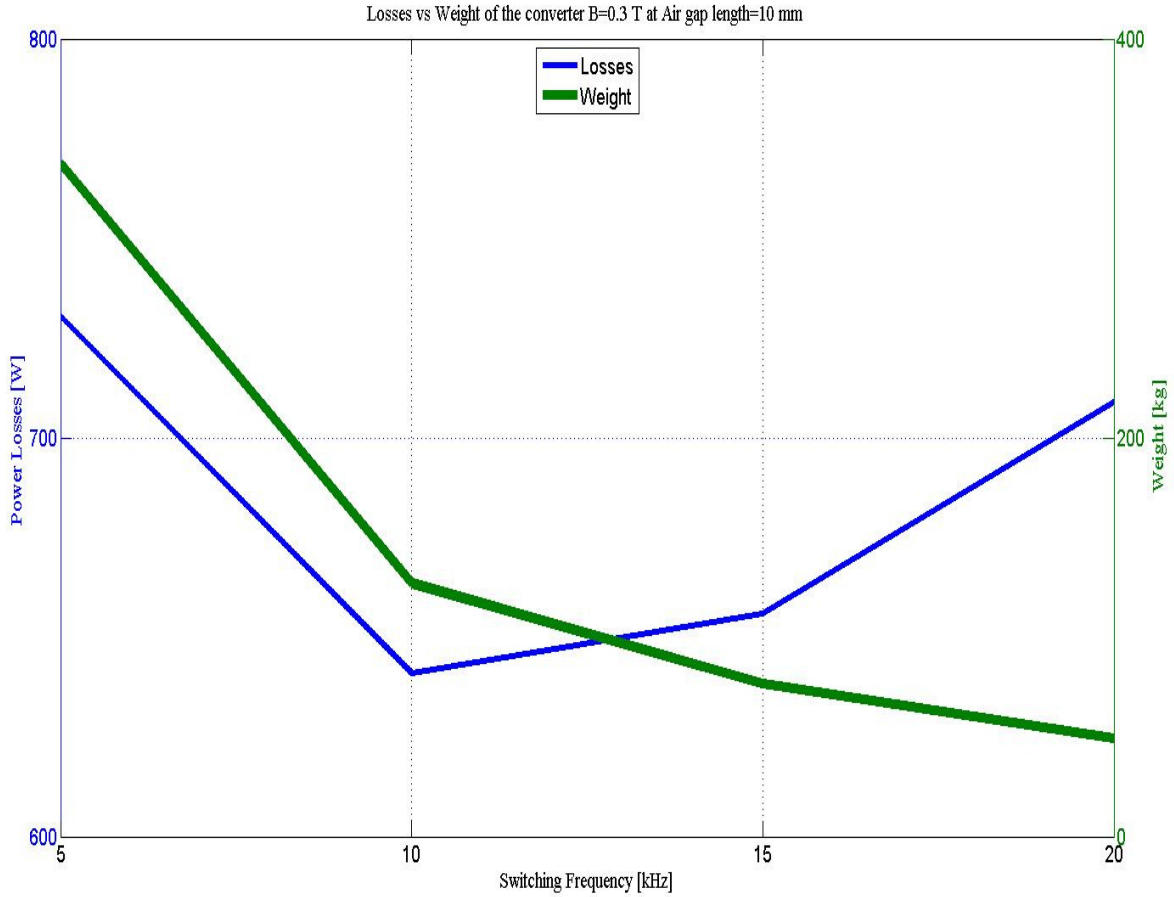

Figure 7.2.Total losses vs. weight of the converter at different frequencies.

As can be seen from Figure 7.2, the total losses of the converter varies from 730 W to 710 W at different switching frequencies and the total weight of the converter varies from 49 kg to more than 300 kg, as can be seen that the cross point of the graph is at around 12.5 kHz switching frequency, where the loss curve cuts the weight.

Generating mode (Buck operation) when B=0.3 T, Lair=10 mm at 10 & 20 kHz:

Figure 7.3 shows the switching, condution losses of IGBT, diode , inductor and efficiency at different loading of the converter.

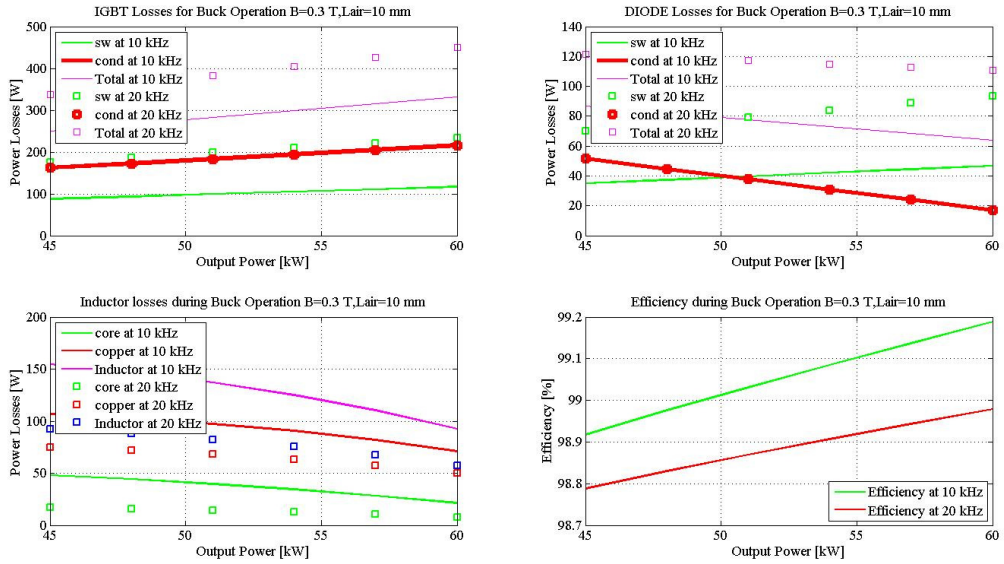

Figure 7.3. IGBT, diode, inductor losses and efficiency plots at different frequencies.

As can be seen from Figure 7.3 that the IGBT conduction losses are increasing as increase in load of the converter where as in diode conduction losses are decreasing as increasing load, during generating mode the total inductor losses are decreasing on both switching frequencies, the total efficiency varies from 99 to 99.2 %.

Figure 7.4 shows the variation between total losses of the converter and the weight of the converter according to the switching frequencies.

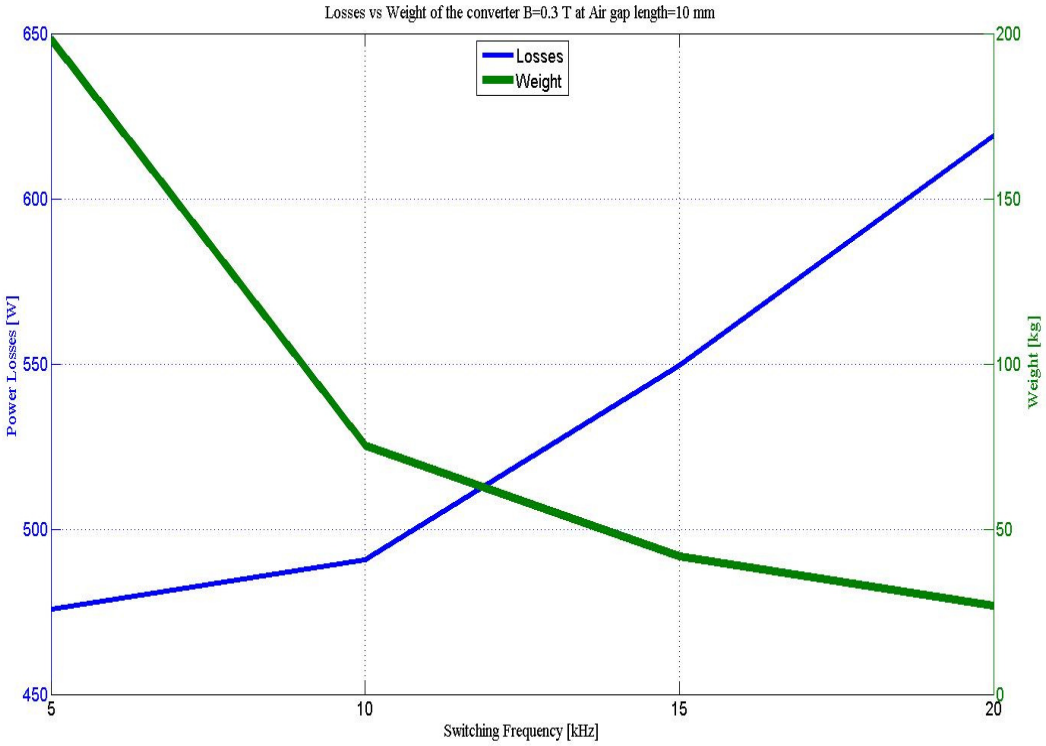

Figure 7.4. Total losses vs. weight of the converter at different frequencies.

As can be seen from Figure 7.4 that the total losses and weight of the converter is smaller compare to the motoring mode of operation.

Again, in Figures 7.5 to 7.33 the same pattern can be observed with slight changes at different load conditions, core materials, core shapes and voltages with different switching frequencies.

Case 1.2: Ferrite material, (ETD-59) for (450V System)

Motoring mode (Boost operation) when B=0.3 T, Lair=10 mm at 10 & 20 kHz:

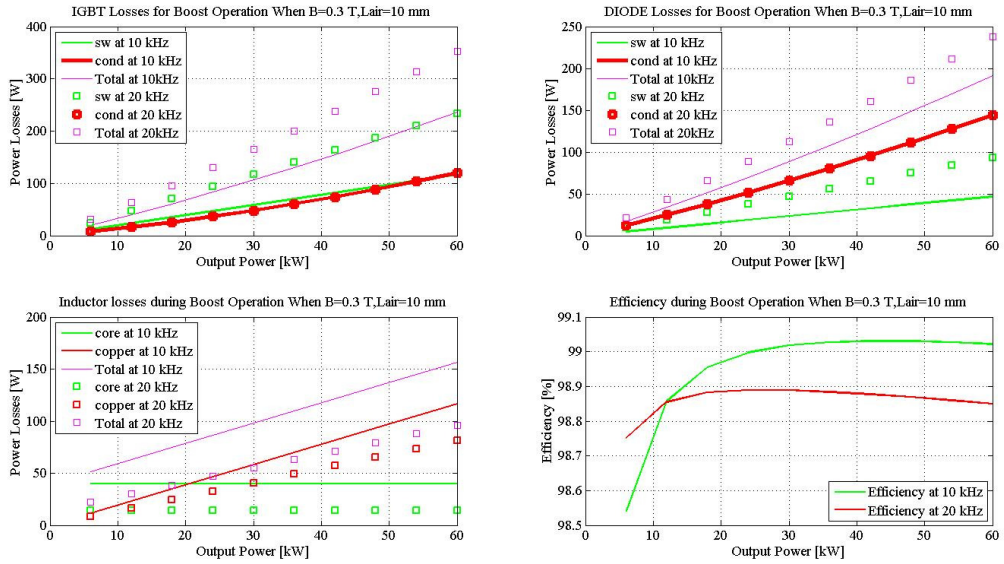

Figure 7.5. IGBT, diode, inductor losses and efficiency plots at different frequencies.

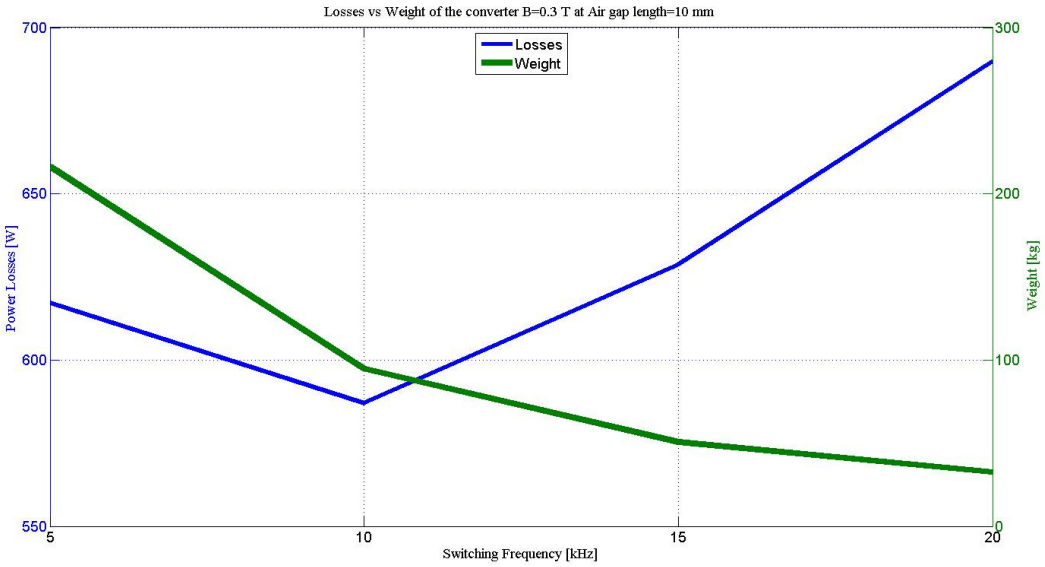

Figure 7.6. Total losses vs. weight of the converter at different frequencies.

Generating mode (Buck operation) when B=0.3 T, Lair=10 mm at 10 & 20 kHz:

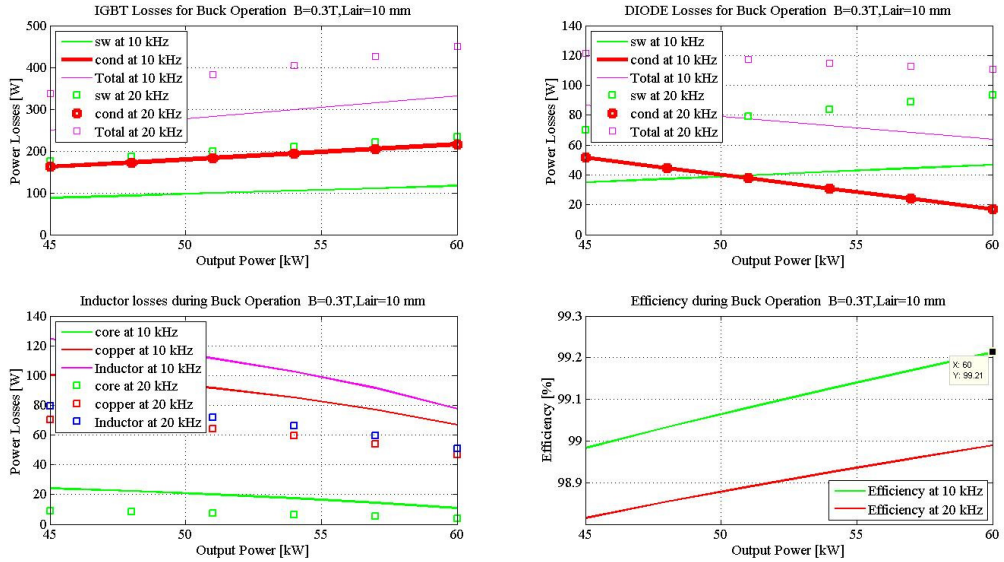

Figure 7.7. IGBT, diode, inductor losses and efficiency plots at different frequencies.

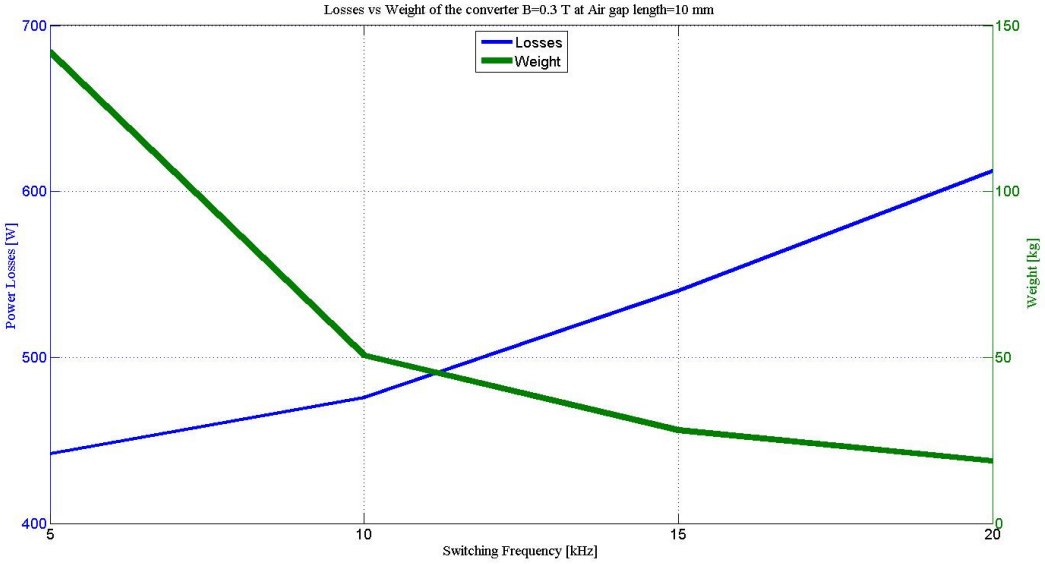

Figure 7.8. Total losses vs. weight of the converter at different frequencies.

Case 1.3: Ferrite material, (EC-70) for (900V System)

Motoring mode (Boost operation) when B=0.3 T, Lair=10 mm at 10 & 20 kHz:

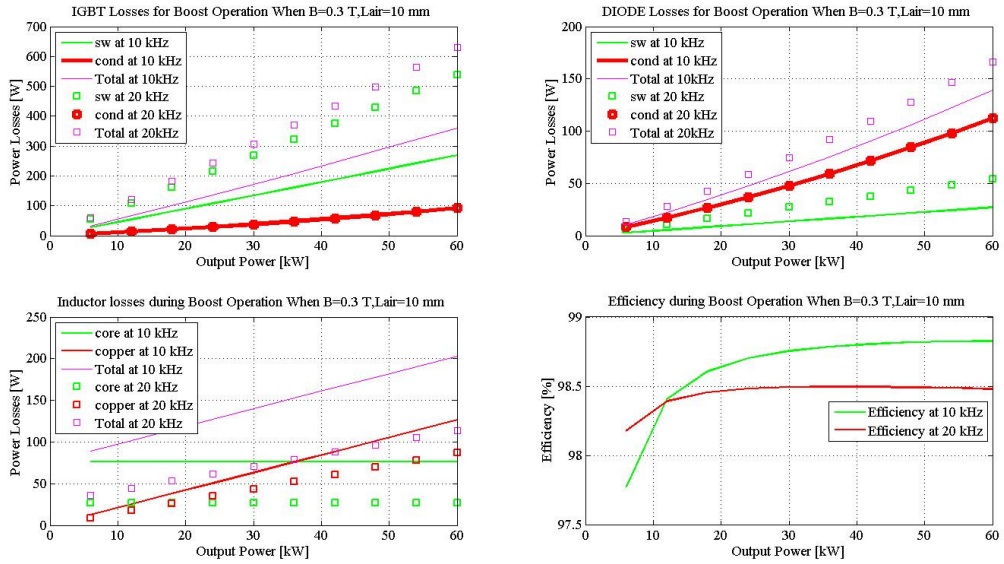

Figure 7.9. IGBT, diode, inductor losses and efficiency plots at different frequencies.

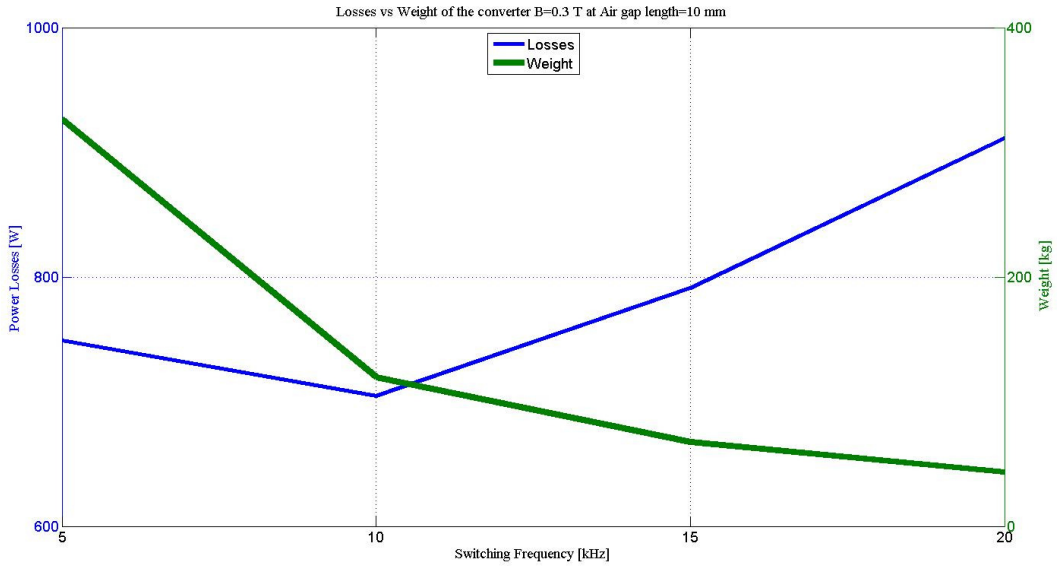

Figure 7.10. Total losses vs. weight of the converter at different frequencies.

Generating mode (Buck operation) when B=0.3 T, Lair=10 mm at 10 & 20 kHz:

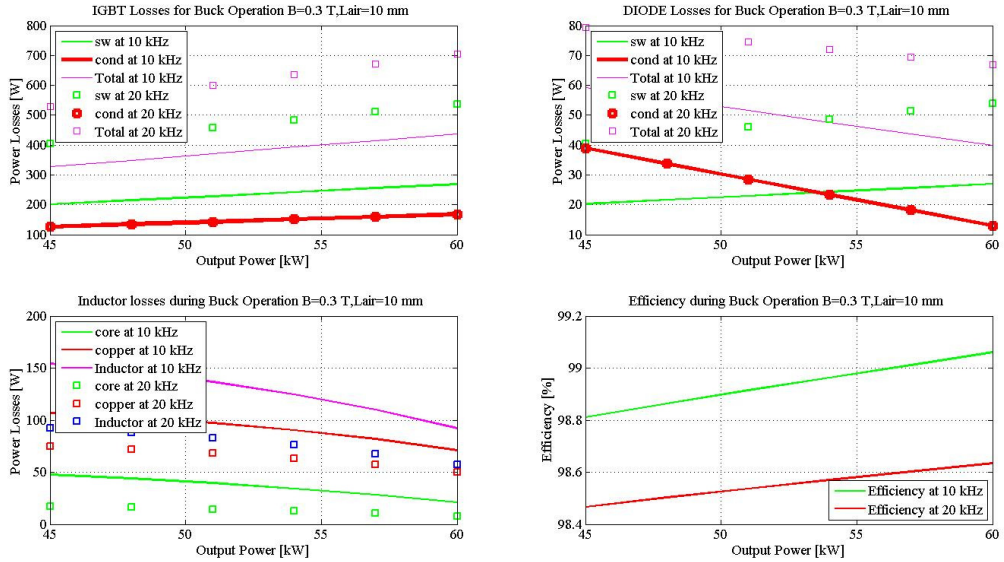

Figure 7.11. IGBT, diode, inductor losses and efficiency plots at different frequencies.

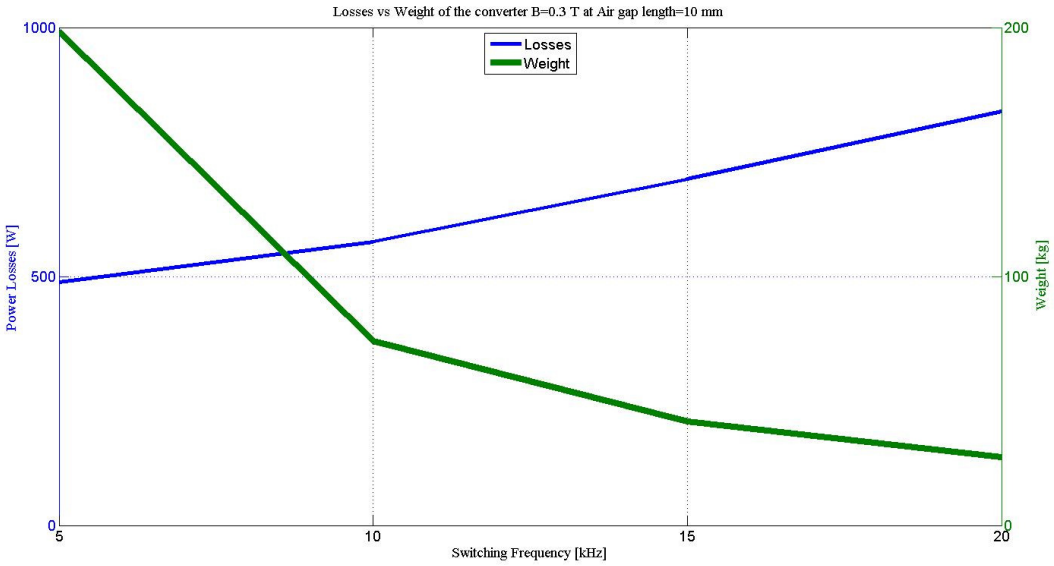

Figure 7.12. Total losses vs. weight of the converter at different frequencies.

Case 1.4: Ferrite material, (ETD-59) for (900V System)

Motoring mode (Boost operation) when B=0.3 T, Lair=10 mm at 10 & 20 kHz:

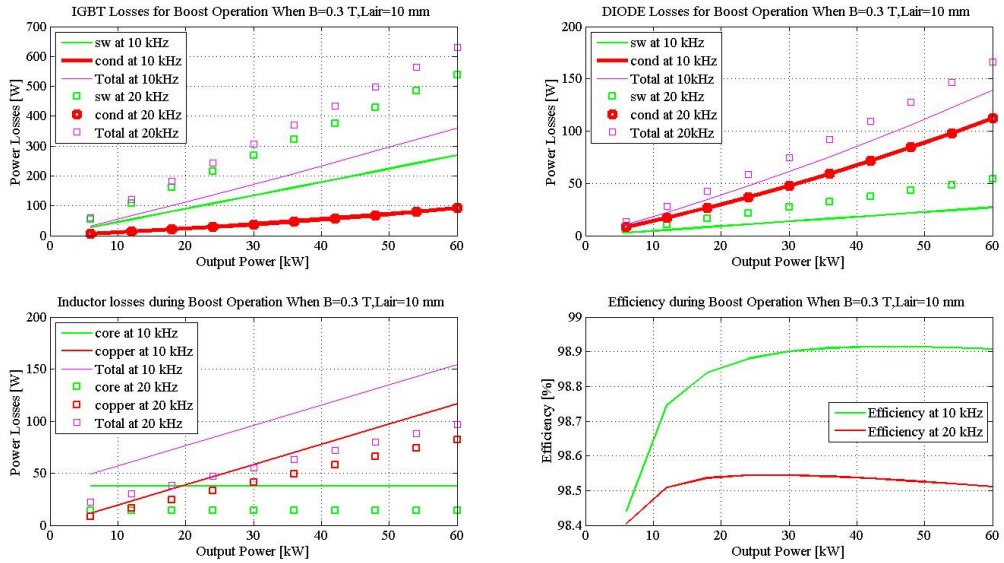

Figure 7.13. IGBT, diode, inductor losses and efficiency plots at different frequencies.

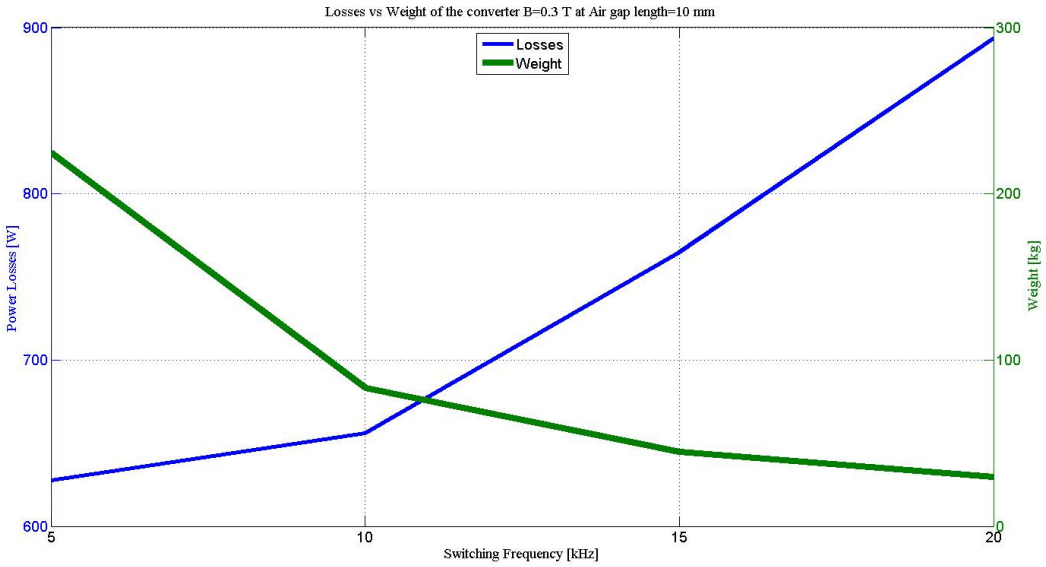

Figure 7.14. Total losses vs. weight of the converter at different frequencies.

Generating mode (Buck operation) when B=0.3 T, Lair=10 mm at 10 & 20 kHz:

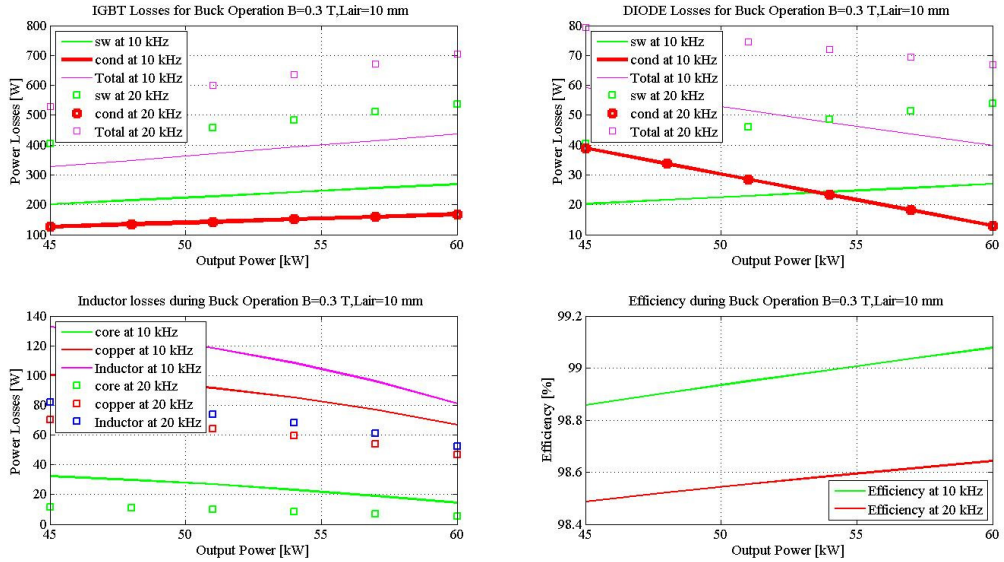

Figure 7.15. IGBT, diode, inductor losses and efficiency plots at different frequencies.

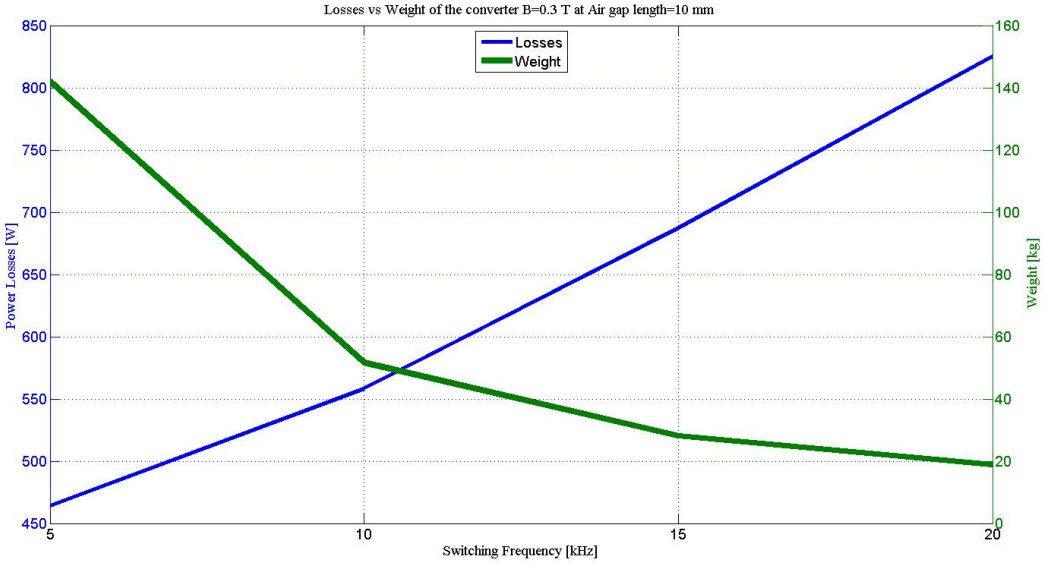

Figure 7.16. Total losses vs. weight of the converter at different frequencies.

Case 2.1: Iron powder material, (EC-70) for (450V System)

Motoring mode (Boost operation) when B=0.5 T, Lair=10 mm at 10 & 20 kHz:

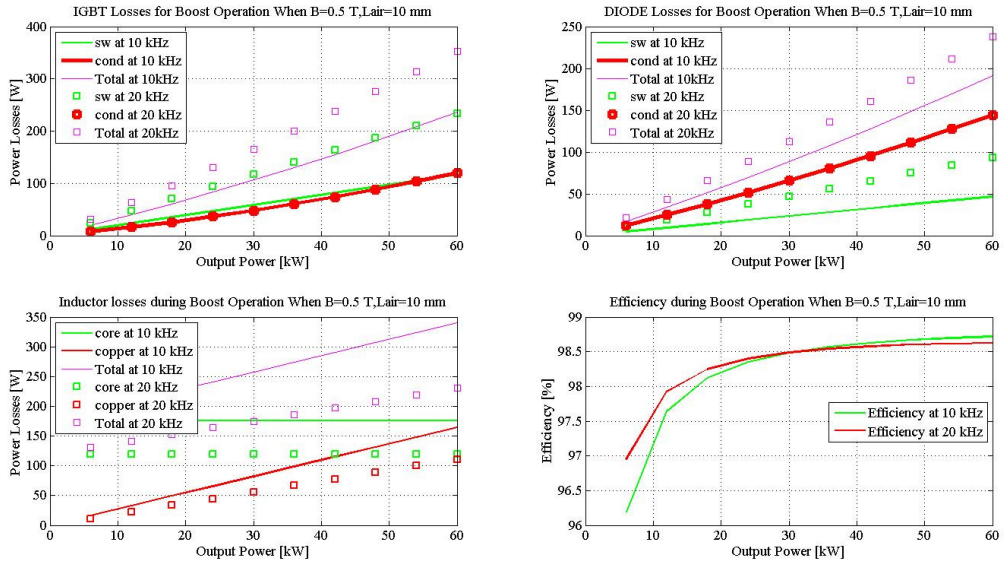

Figure 7.17. IGBT, diode, inductor losses and efficiency plots at different frequencies.

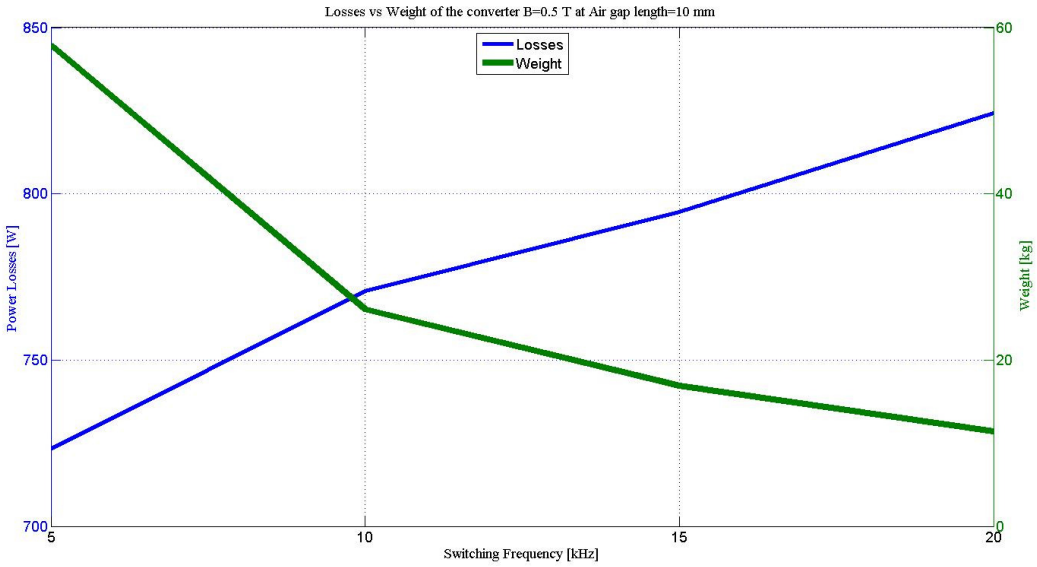

Figure 7.18. Total losses vs. weight of the converter at different frequencies.

Generating mode (Buck operation) when B=0.5 T, Lair=10 mm at 10 & 20 kHz:

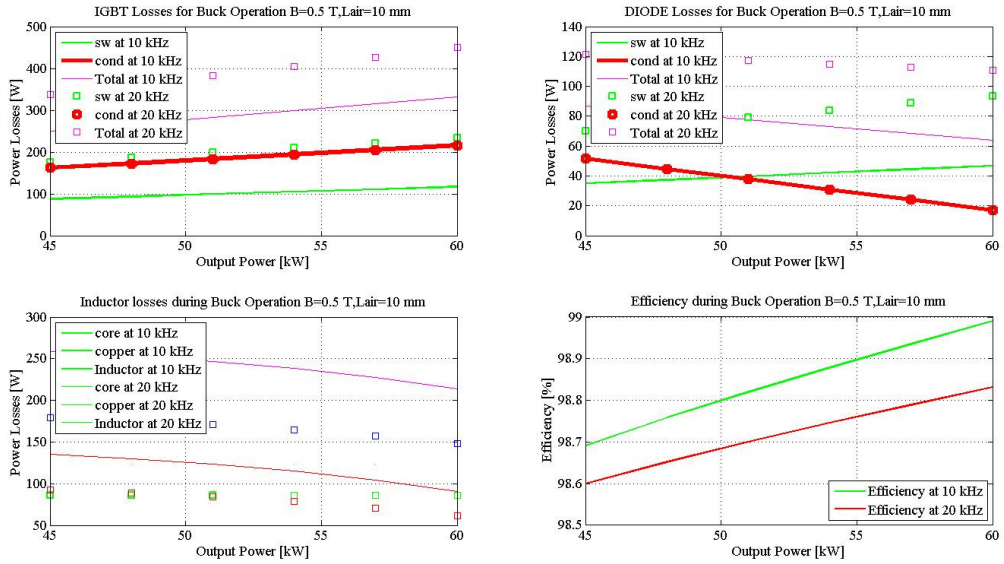

Figure 7.19. IGBT, diode, inductor losses and efficiency plots at different frequencies.

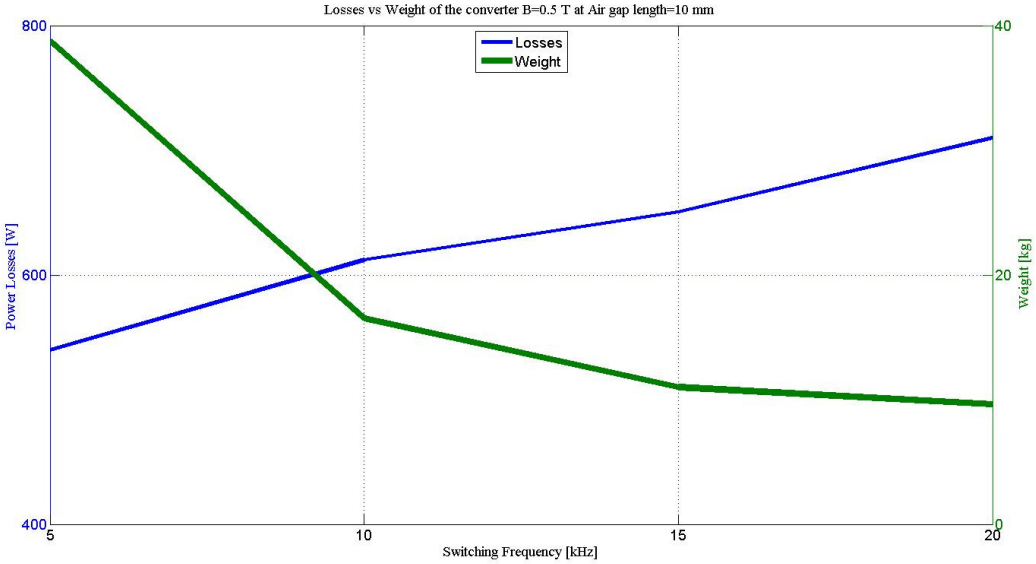

Figure 7.20. Total losses vs. weight of the converter at different frequencies.

Case 2.2: Iron powder material, (ETD-59) for (450V System)

Motoring mode (Boost operation) when B=0.5 T, Lair=10 mm at 10 & 20 kHz:

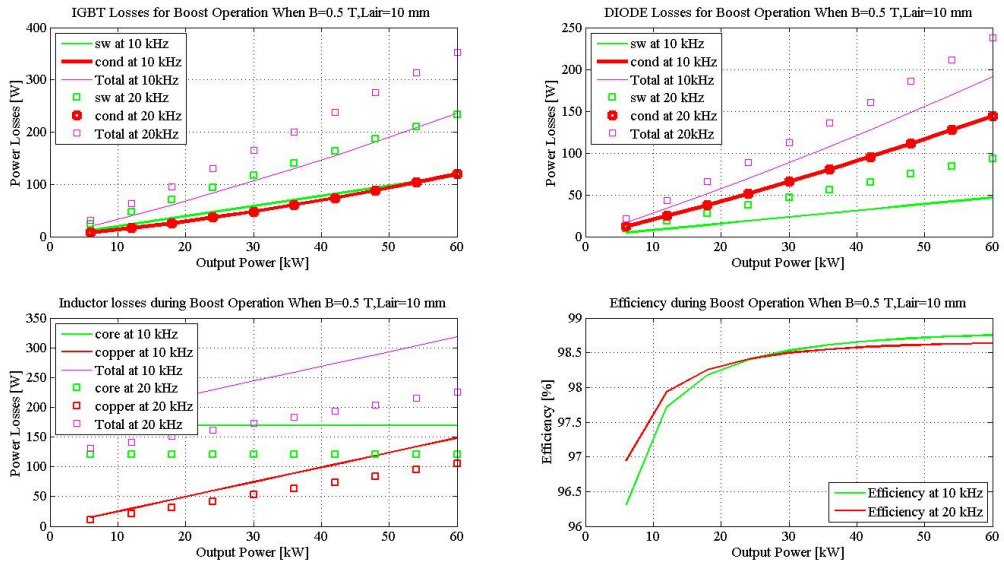

Figure 7.21. IGBT, diode, inductor losses and efficiency plots at different frequencies.

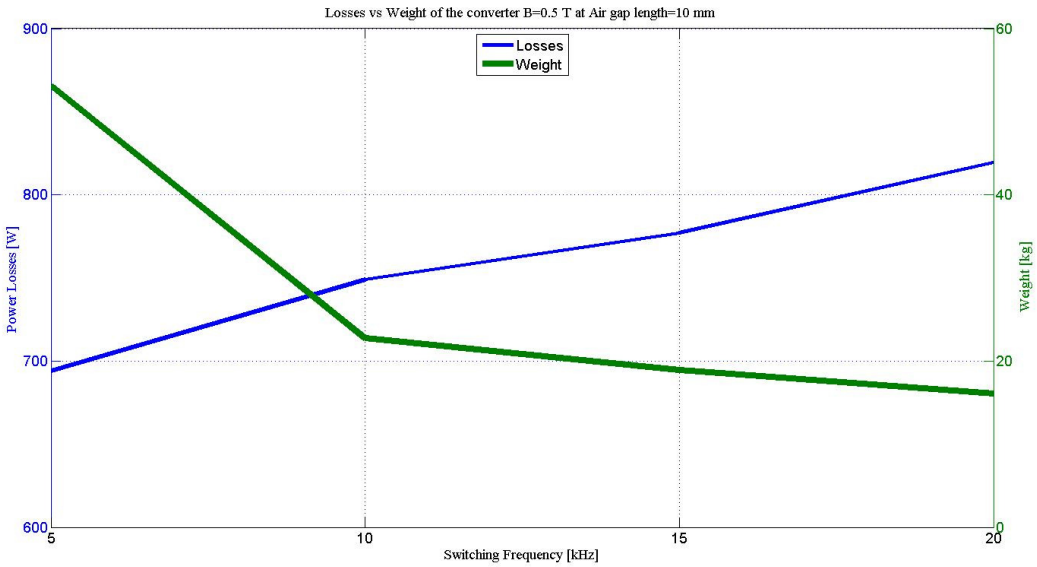

Figure 7.22. Total losses vs. weight of the converter at different frequencies.

Generating mode (Buck operation) when B=0.5 T, Lair=10 mm at 10 & 20 kHz:

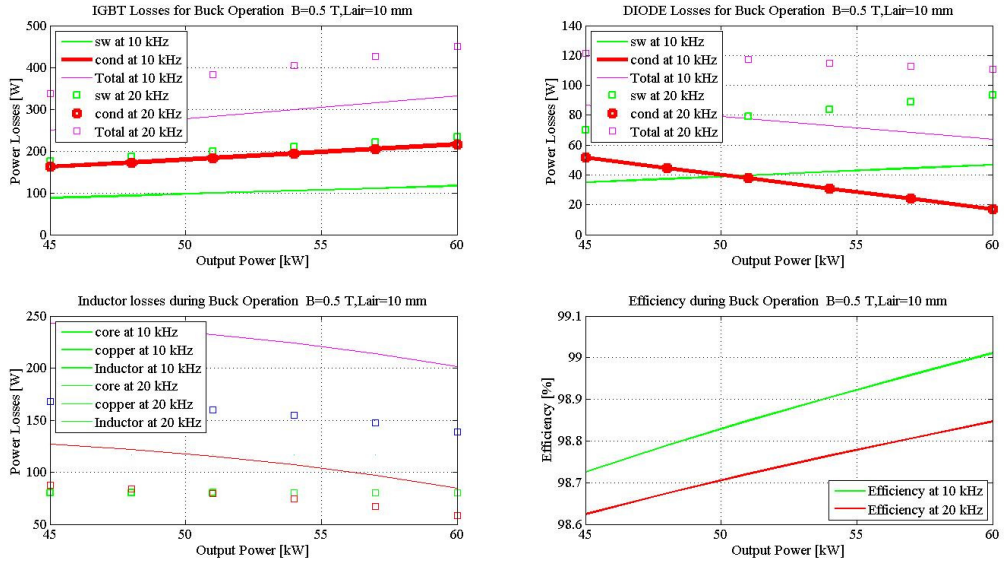

Figure 7.23. IGBT, diode, inductor losses and efficiency plots at different frequencies.

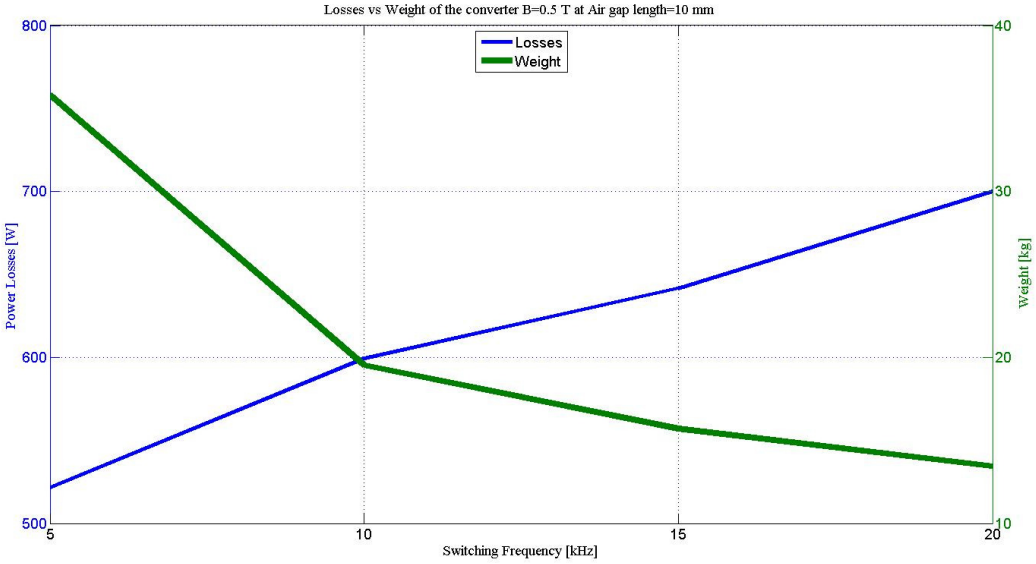

Figure 7.24. Total losses vs. weight of the converter at different frequencies.

Case 2.3: Iron powder material, (EC-70) for (900V System)

Motoring mode (Boost operation) when B=0.5 T, Lair=10 mm at 10 & 20 kHz:

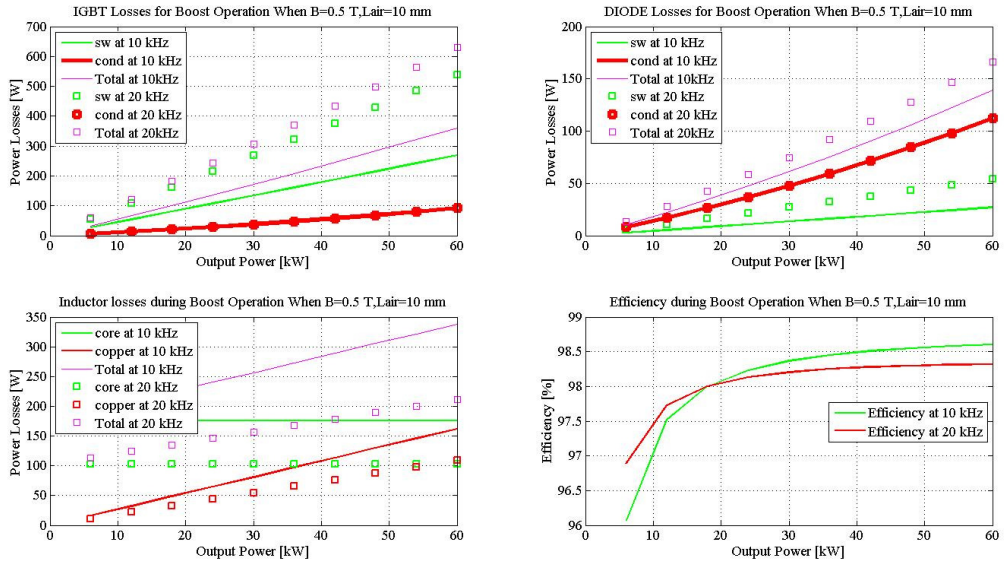

Figure 7.25. IGBT, diode, inductor losses and efficiency plots at different frequencies.

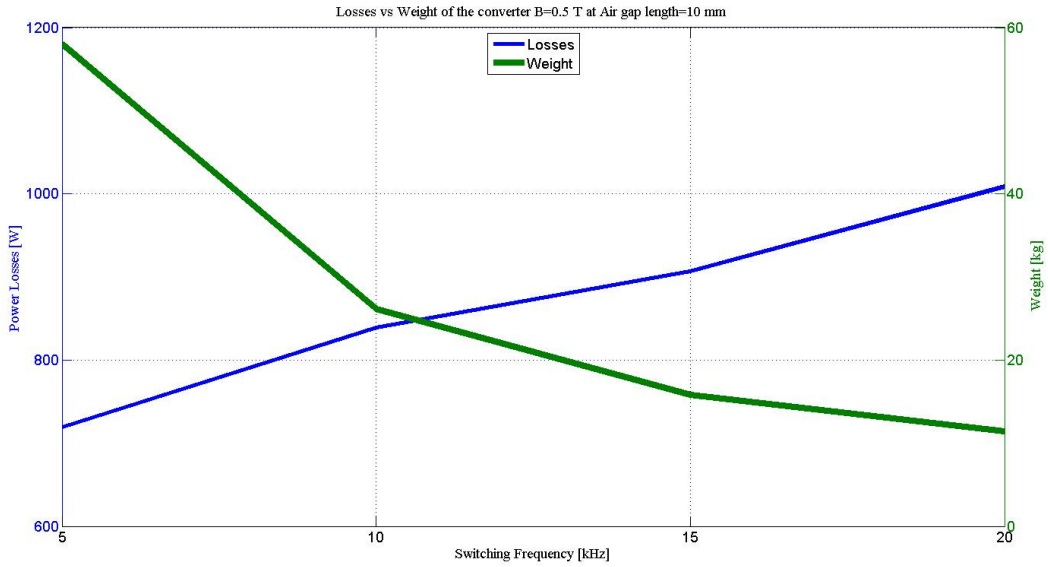

Figure 7.26. Total losses vs. weight of the converter at different frequencies.

Generating mode (Buck operation) when B=0.5 T, Lair=10 mm at 10 & 20 kHz:

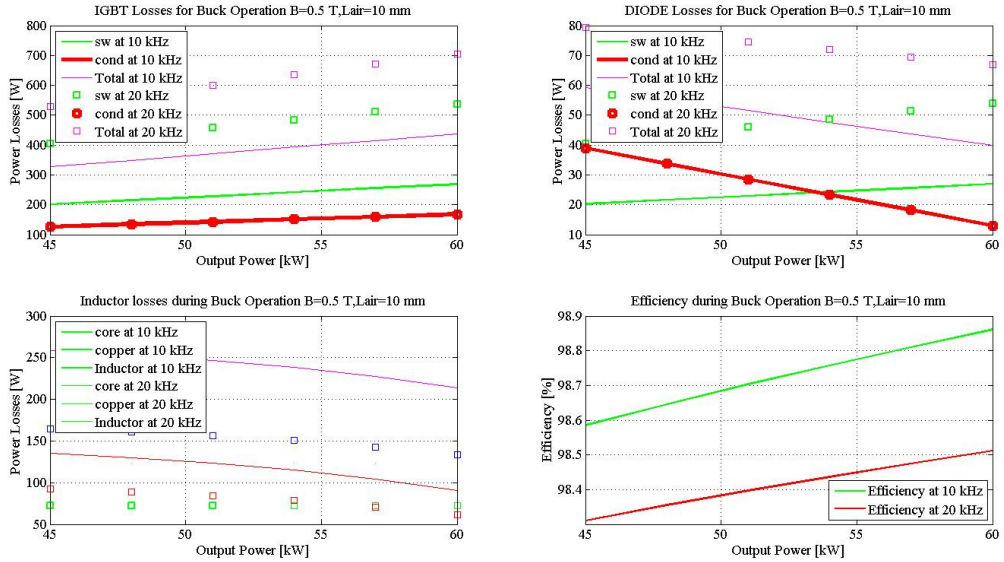

Figure 7.27. IGBT, diode, inductor losses and efficiency plots at different frequencies.

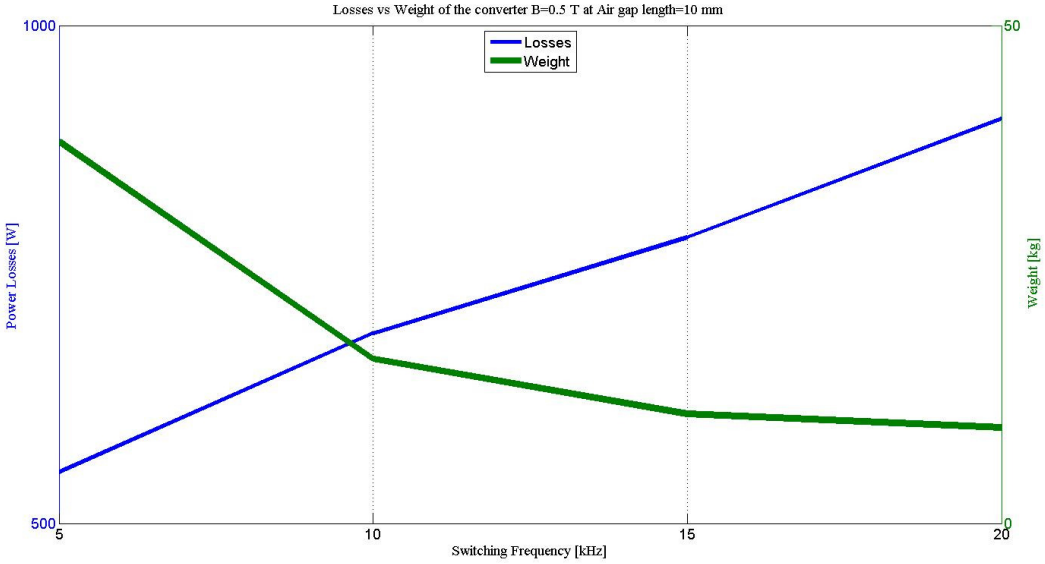

Figure 7.28. Total losses vs. weight of the converter at different frequencies.

Case 2.4: Iron powder material, (ETD-59) for (900V System)

Motoring mode (Boost operation) when B=0.5 T, Lair=10 mm at 10 & 20 kHz:

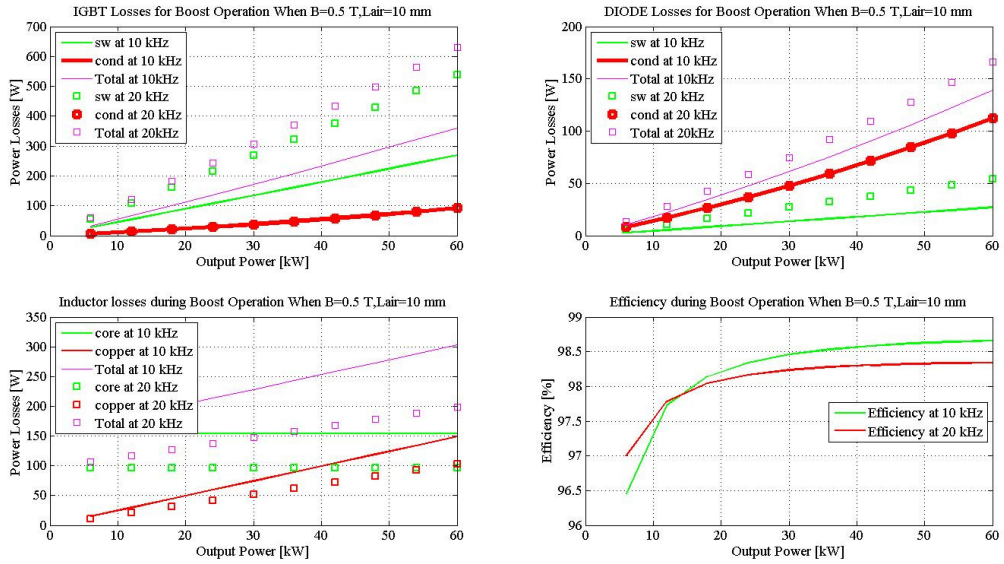

Figure 7.29. IGBT, diode, inductor losses and efficiency plots at different frequencies.

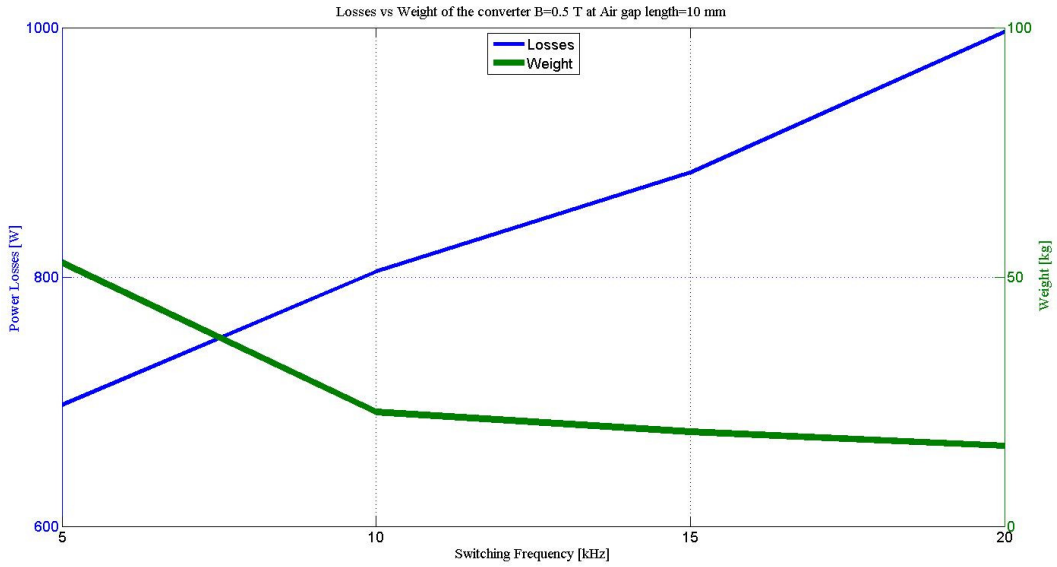

Figure 7.30. Total losses vs. weight of the converter at different frequencies.

Generating mode (Buck operation) when B=0.5 T, Lair=10 mm at 10 & 20 kHz:

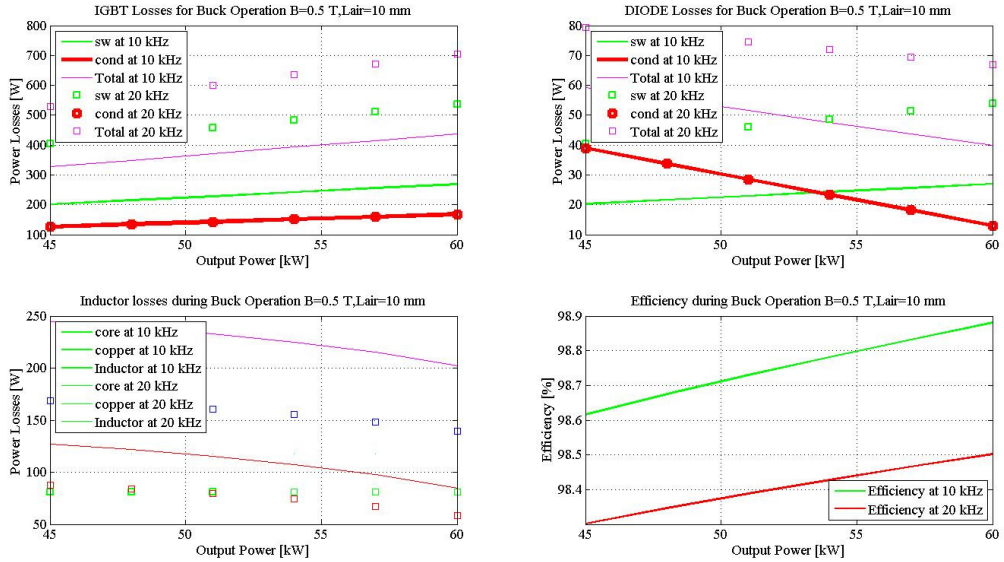

Figure 7.31. IGBT, diode, inductor losses and efficiency plots at different frequencies.

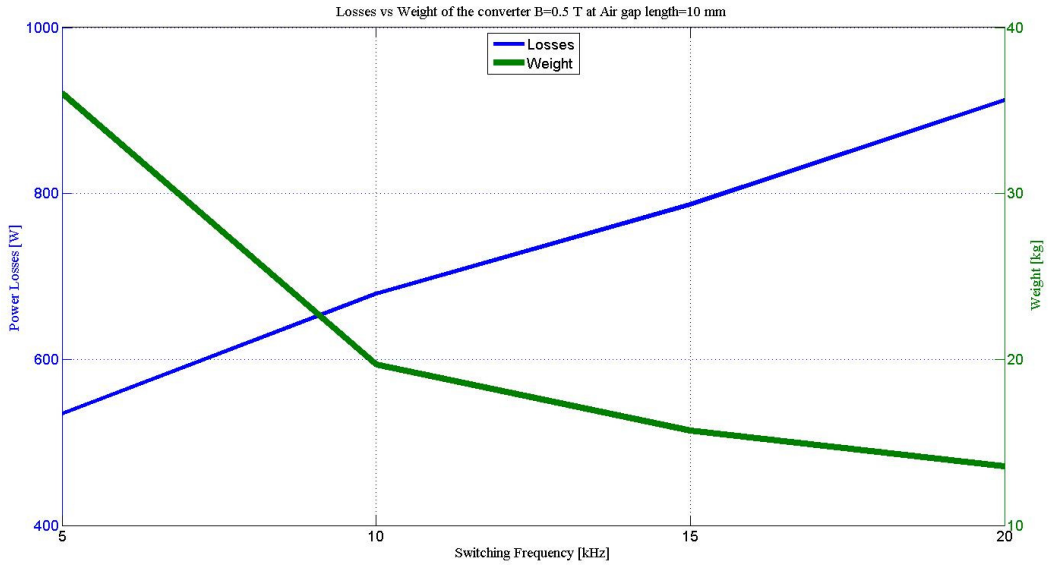

Figure 7.33. Total losses vs. weight of the converter at different frequencies.

In Table 7.1 and 7.2 the results of motoring mode and generating mode are presented at 450 V.

Table 7.1. Summary of results for motoring operation at 450 V.

Core shape and materials	Losses (W)		Weight (kg)		Inductance L (uH)		No. of turns N		Flux density B (T)		Efficiency η (%)		Fill factor (%)	
	Switching frequency (kHz)													
	10	20	10	20	10	20	10	20	10	20	10	20	10	20
Ferrite EC-70	641	709	127	50	500	250	13	12	0.3	0.3	98.93	98.81	3	6
Ferrite ETD-59	587	690	94.77	32.50	500	250	12	12	0.3	0.3	99.02	98.85	5	11
Iron powder EC-70	771	795	26.08	11.39	500	250	36	32	0.5	0.5	98.71	98.62	48	75
Iron powder ETD-59	750	820	22.74	16.09	500	250	43	27	0.5	0.5	98.75	98.63	75	75

Table 7.1. Summary of results for generatin operation at 450 V.

Core shape and materials	Losses (W)		Weight (kg)		Inductance L (uH)		No. of turns N		Flux density B (T)		Efficiency η (%)		Fill factor (%)	
	Frequency (kHz)													
	10	20	10	20	10	20	10	20	10	20	10	20	10	20
Ferrite EC-70	491	619	75.27	26.75	700	300	18	17	0.3	0.3	99.18	98.97	5	10
Ferrite ETD-59	476	613	50.18	18.81	700	300	17	16	0.3	0.3	99.21	98.98	8	16
Iron powderEC-70	612	710	16.51	9.63	700	399	47	38	0.5	0.5	98.99	98.83	63	75
Iron powderETD-59	600	700	19.53	13.44	700	300	41	32	0.5	0.5	99.01	98.84	75	75

The summary of results from both motoring and generating mode of operation taking into account at 450 V system and show the losses, weight, inductance, number of turns peak flux density, efficiency, fill factor with different core material, core shapes, at different switching frequencies.

And , the red and orange marked in Table 7.1 show how the losses, weight and efficiency varies according to different parameters.

In Table 7.3 and 7.4 the results of motoring mode and generating mode are presented at 900 V.

Table 7.3. Summary of results for motoring operation at 900 V.

Core shape and materials	Losses (W)		Weight (kg)		Inductance L (uH)		No. of turns N		Flux density B (T)		Efficiency η (%)		Fill factor (%)	
	Frequency (kHz)													
	10	20	10	20	10	20	10	20	10	20	10	20	10	20
Ferrite EC-70	705	911	119.53	43.37	2000	1000	26	25	0.3	0.3	98.82	98.48	3	7
Ferrite ETD-59	656	894	83.26	29.50	2000	1000	25	25	0.3	0.3	98.90	98.51	6	12
Iron powderEC-70	840	1000	26.15	11.42	2000	1000	71	63	0.5	0.5	98.60	98.31	48	75
Iron powderETD-59	805	831	73.93	27.43	2000	1000	68	53	0.5	0.5	98.65	98.33	75	75

Table 7.4. Summary of results for generating operation at 900 V.

Core shape and materials	Losses (W)		Weight (kg)		Inductance L (uH)		No. of turns N		Flux density B (T)		Efficiency η (%)		Fill factor (%)	
	Frequency (kHz)													
	10	**20**	**10**	**20**	**10**	**20**	**10**	**20**	**10**	**20**	**10**	**20**	**10**	**20**
Ferrite EC-70	570	830	73.93	24.43	2700	1300	35	34	0.3	0.3	99.05	98.63	5	9
Ferrite ETD-59	559	825	51.61	18.18	2700	1300	34	34	0.3	0.3	99.07	98.64	8	16
Iron powder EC-70	691	906	16.51	9.63	2700	1300	92	75	0.5	0.5	98.86	98.51	63	74
Iron powder ETD-59	680	912	19.68	13.55	2700	1300	82	64	0.5	0.5	98.88	98.70	75	75

Again the same pattern can be observed: The 900 V system has higher losses, weight and lower efficiency.

And, the gray marked coulmns in Table 7.1, 7.2, 7.3 and 7.4 shows the fill factor of winding i.e, not feasible for any practical design. The idea here is to show the difference, if the same air gap length maintained in both core materials.

8 CONCLUSION

In this thesis, DC-DC converter is investigated with different core materials, core shapes, different voltage levels (450 and 900V) and at two different frequencies (10 and 20 kHz) for a EV/BEV/HEV.

- The efficiency of the converter is higher for a ferrite material when the ETD-59 core shape is used as compared with EC-70 core shape is used for both voltage levels.
- The weight of the converter with ferrite material is lower for the ETD-59 core shape for both voltage systems.
- The 450 V system is better than 900 V system with ferrite core material.
- The efficiency of the converter is higher for iron powder material when the ETD-59 core shape is used as compared EC-70 core shape for both voltage levels.
- The weight of the converter with ferrite material is lower for the EC-70 core shape for both voltage systems.
- The 450 V system is better than the 900 V system with iron powder core material.
- For lower airgap lengths the fill factor is not feasible with ferrite core material.

Hence the design of DC-DC converter with the EC-70 core shape, iron powder material, 450 V system at 20 kHz is better.

The future work is to implement the converter in Matlab Simulink and more over, to validate with the practical design.

REFERENCES

[1] Mi, C., Peng, F.Z., Kelly, K.J., O'Keefe, M. and Hassani, V. (2008), `Topology, design, analysis and thermal management of power electronics for hybrid electric vehicle applications', Int. J. Electric and Hybrid Vehicles. Vol. 1, No. 3, pp.276±294.

[2] Edition 2009-01-29, Published by Infineon Technologies AG, Am Campeon 1-12, 85579 Neubiberg, Germany, © Infineon Technologies AG 2006.

[3] http://en.wikipedia.org/wiki/Lithium-ion_battery

[4] David Linden, Thomas B. Reddy (ed). *Handbook Of Batteries 3rd Edition*. McGraw-Hill, New York, 2002 ISBN 0-07-135978-8 chapter 35

[5] http://www.mitsubishi-otors.com/corporate/about_us/technology/review/e/pdf/2003/15E_10.pdf

[6] Mohan, Undeland, Robbins; 'Power Electronics Converters, applications and design, media enhanced third edition, John Wiley & sons, Inc., pp. 760-767

[7] http://igbt.cn/admin/productfile/BSM300GB60DLC.pdf

[8] http://www.hipih.com/SMC/datasheet/SMC_gWBPuycesVEfh.htm